International Journal of Peptide Research and Therapeutics (2022) 28:71
https://doi.org/10.1007/s10989-022-10380-7

A Novel Multiepitope Vaccine Against Bladder Cancer Based on CTL and HTL Epitopes for Induction of Strong Immune Using Immunoinformatics Approaches

Ehsan Jahangirian[1] · Ghadir A. Jamal[2] · MohammadReza Nouroozi[3] · Alemeh Mohammadpour[1]

Accepted: 7 February 2022 / Published online: 24 February 2022

Abstract
Bladder cancer is well-known cancer in two forms of muscle-invasive and non-muscle-invasive bladder cancer which is responsible for annual deaths worldwide. Common therapies methods are somewhat successful; however, these methods have the limitations such as the side effects of chemotherapy which necessitate the requirement for new preventive methods against bladder cancer. Hence, we explain a novel designed multi-epitope vaccine against bladder cancer using the immunoinformatics tool. Three well-known BLCAP, PRAM, and BAGE4 antigens were evaluated due to most repetitive CTL and HTL epitopes binding. IFNγ and IL10 inducer potential of selected epitopes were investigated, as well as liner and conformational B-cell epitopes. Human beta-defensin 3 and PADRE sequence were added to construct as adjuvants, along with EAAAK, AAY, and GGGS linkers to fuse CTL and HTL epitopes. Results showed this construct encodes a soluble, non-toxic, and non-allergic protein with 70 kDa molecular weight. Modeled 3D structure of vaccine was docked whit Toll-Like Receptors (TLR) of 7/8. Docking, molecular dynamics simulation and MMBPSA analysis confirmed stability of vaccine-TLR complexes. The immunogenicity showed this construct could elicit humoral and cellular immune responses. In silico and immunoinformatics evaluations suggest that this construct is a recombinant candidate vaccine against bladder cancer.

Keywords Bladder cancer · Immunoinformatics · Molecular docking · Molecular dynamics · Multi-epitope vaccine

Introduction

Bladder cancer is common cancer worldwide known for two forms of muscle-invasive and non-muscle-invasive bladder cancer (NMIBC) (Jiang et al. 2020; Lenis et al. 2020; Slovacek et al. 2021). Although the type of muscle-invasive bladder cancer is more dangerous, NMIBC type requires more preventative treatment because of higher recurrence rate and longer and more costly care (Shore et al. 2021). These preventative treatments include cystoscopies and transurethral resection (TUR), intravesical chemotherapy, and immunotherapy (Melekos and Moutzouris 2000; Fang and Huang 2009). One successful way is using Bacillus Calmette–Guérin (BCG) vaccine intravesical immunotherapy, which decreased the risk of recurrence and progression of NMIBCs (Shelley et al. 2000). The intrauterine injection of BCG causes extensive inflammation in the bladder wall which helps kill tumor cells, but BCG intravesical immunotherapy may have short-term immune-stimulating effects (Bevers et al. 2004). The recurrence of bladder cancer increases the cost of treatment, as well as the side effects of using chemotherapy drugs in the process of treating bladder cancer, today clinical studies is given in priority to discover effective, cost-effective, and accurate treatment strategies such as utilization of cytotoxicity properties of nanoparticles in the direction of suppressing the expression of cancer antigens and metastasis of cancer cells (Yin et al. 2016; DeGeorge et al. 2017; Hosseini et al. 2019).

Ehsan Jahangirian and Ghadir A. Jamal are joint first authors (equally contributed).

✉ Ghadir A. Jamal
ghadir.jamal@ku.edu.kw

[1] Department of Animal Biotechnology, National Institute of Genetic Engineering and Biotechnology (NIGEB), Tehran, Iran

[2] Faculty of Allied Health Sciences, Kuwait University, Kuwait, Kuwait

[3] Department of Animal Science and Food Technology, Agriculture Science and Natural Resources University Khouzestan, Ahwaz, Iran

Antibody therapy is one of the well-known methods against cancerous tumors. However, administration of monoclonal antibodies may cause adverse side effects due to their accumulation in non-target organs. Nikpoor et al. (2015) succeeded in using encapsulated monoclonal antibodies in Nano-liposomes as a model antibody for intravenous immunoglobulin (IVIG) in mice bearing C-26 colon carcinoma tumors, to make the efficiency of PEGylated liposomes more efficient in delivering antibodies to the tumor site than non-PEGylated liposomes (Nikpoor et al. 2015).

Non-invasive bladder cancer is dangerous in which it may not be of interest to the patient because it may not cause pain or early detection in the early stages and may progress easily, as well as the risk of developing secondary primary tumors also follows (Lenis et al. 2020). Chemotherapy drugs are commonly used as antibiotics or anti-cancer drugs, but they often affect normal human cells which have serious side effects (Koch et al. 2021). Moreover, cancer cells can escape chemotherapeutic agents with cellular changes (Schirrmacher 2019).

The first barrier to bladder infection and cancerous tissue cancer is asymmetric umbrella cells around the urinary tract (Romih et al. 2005). Due to their apical membrane, these umbrella cells form an impermeable shell covered with layers of glycan's against the penetration of bacteria and other pathogens and ultimately cause the urothelium to benefit from a highly paradigmatic mucosal defense system (Veranic et al. 2004; Khandelwal et al. 2009). However, a very important cellular immune response dependent on TLRs plays a key role in combating pathogens and carcinogens (Kawai and Akira 2007; Ohadian Moghadam and Nowroozi 2019). Today, it was shown that activating TLRs by their agonists triggers immune response mediators such as cytokines, chemokines that help eliminate the cellular infection (Adams 2009; Hennessy et al. 2010; Urban-Wojciuk et al. 2019). In general, TLR5 is poorly expressed in normal bladder cells. TLR2, TLR3, and TLR7 are moderately expressed, and finally, TLR9 and TLR4 are strongly expressed (Ohadian Moghadam and Nowroozi 2019). Although TLRs have a courtly role in fighting cancer cells, including bladder cancer, but they act dually due to their ability to regulate immune responses (LaRue et al. 2013a). It was shown that TLR2, TLR3, TLR4, TLR5, TLR7, and TLR9 levels of expression in normal bladder cells are very high, while their levels of expression in bladder cancer cells are reduced (So and Ouchi 2010). But research has shown that cytokines and chemokines involved in the activation of some TLRs may contribute to bladder cancer progression (Vasekar et al. 2016; Wołącewicz et al. 2020). The low-grade bladder cancer cell line (MGH-U3) shows similar inflammatory responses in the imitation of grade 1 NMIBC bladder cancer in decreased expression with TLR (LaRue et al. 2013b; Ohadian Moghadam and Nowroozi 2019). Studies showed BCG treatment of superficial urothelial cancer (UC) leaded to activation of apoptosis in UC (Yu et al. 2015). Moreover, phagocytosis-related markers and interleukin-1 receptor-associated kinases 2 and 4 were increased when TSGH8301 cells, low-grade UC cells, were treated by BCG (Yu et al. 2015). Increasing the expression of TLR7 by activating protein kinases activated by mitogen ERK and JNK provides the conditions that lead to tumor escape via the inhibition of T cell immunity during bladder cancer and contributes to the progression of cancer (Chi et al. 2017). However, the stimulation of TLR2 agonists triggers the release of pro-inflammatory cytokines that impair bladder cancer progression. Although TLRs are much more pronounced in normal urinary cells, their stable expression and activity in tumor cells make it possible to use TLR ligands for treatment. For example, the success of TLR-mediated BCG immunotherapy for NMIBCs suggests that TLR-based alternative immunotherapy may also be successful for these cancers.

In many studies, the role of TLR agonists to stimulate cellular immunity was indicated. Recently, a new agonist called Beta-defensin 3 was introduced for TLRs (Funderburg et al. 2007). Studies showed that Beta-defensin 3 can effectively activate dendritic cells (DCs) and helper T cells (Th)-1, increase the expression levels of CD40, CD80, and CD86 molecules, MHC I and II classes, and IL-pre-inflammatory cytokines (Tani et al. 2000; Ferris et al. 2013). IL-12, IL-1β, TNF-α, as well as stimulation of DC migration capacity in vitro and in vivo (Semple et al. 2010; Jiang et al. 2012; Bian et al. 2017). This ultimately improves DC-based anti-tumor immune system and secretes CD4 (+) and CD8 to secrete IFN-γ and mediate T cellular toxicity and help promote immunosuppressive T-cell therapy vaccines (Joly et al. 2005; Kim et al. 2018).

Several specific antigens are strongly expressed during cancers associated to the urinary system, such as Bladder Cancer (BLCA), and their introduction into the immune system can trigger a specific cellular immune system for bladder cancer (Santoni et al. 2012). BLCA antigens are members of six bladder-specific nuclear matrix proteins (EMPs), which are known as specific urinary markers of bladder cancer (Getzenberg et al. 1996; Santoni et al. 2012). Studies showed BLCA has a role in DNA replication and RNA synthesis of cellular functions, as well as in nuclear morphology, which leads is associated to tumor cell proliferation, survival, and angiogenesis (Berezney and Buchholtz 1981; van Eekelen and van Venrooij 1981; Seddighzadeh et al. 2003). BLCA is expressed in carcinogenesis and tumor, and because of their high sensitivity, they are considered as markers in the diagnosis of bladder cancer (Feng et al. 2011).

PReferentially expressed Antigen of MElanoma (PRAME) is known as an atypical cancer-testis gene which is the high expression in several cancers such as melanoma,

breast cancer, and leukemia. Besides, several studies indicated that testicular cancer-related antigens, such as PRAME, are also expressed in bladder cancer (Dyrskjøt et al. 2012; Kulkarni et al. 2012; Lerut et al. 2015; Xu et al. 2020). The capability of triggering an anti-tumor immune response in a melanoma, along with inducing specific killing of PRAME expressing leukemia cells, has caused PRAME to have great immunogenicity. Several studies confirmed the expression of PRAME in urothelial carcinoma and non-muscle-invasive tumors (Dyrskjøt et al. 2012). It has shown that cancer-testis genes are expressed in bladder cancer, particularly associated with high-grade tumors (Simpson et al. 2005). Utilizing CT antigens such as PRAME as bladder antigen cancer vaccine candidates may ultimately induce an immune response in specific immunotherapy against bladder cancer. We used antigen, expressed in non-muscle-invasive bladder carcinomas to stimulate and identify a specific immune response to bladder cancer.

BAGE is an antigen associated with the human B melanoma antigen and encodes a putative protein of 43 amino acids that are found to be expressed in different tumors (Boël et al. 1995). BAGEL has a pattern of expression similar to the MAGE, GAGE, and LAGE/NY-ESO-1 families, which are highly expressed in urinary cancers (De Plaen et al. 1994; Lethé et al. 1998; De Backer et al. 1999). Immunohistochemistry has identified the antigens in cancers of histological origin, especially bladder cancer and melanoma (Amin 2009; Bellizzi 2020). Moreover, two studies have shown that BAGE is involved in cancer/testis expression profile and is also expressed in bladder carcinoma simultaneously (Boël et al. 1995; Ruault et al. 2002). Using traditional methods of vaccine production is very costly and time-consuming, in addition to the need for repeated tests and errors in the laboratory. Today, it is possible to predict epithelial B-cells and T cells using immunoinformatics tools (Safavi et al. 2019). These tools help achieve a recombinant vaccine that accurately stimulates the cell's immune response (Validi et al. 2018; Beg et al. 2021).

The use of molecular binding studies to predict or confirm experimental results plays an important role in understanding the function of protein–protein, protein-peptide, protein-DNA or protein–ligand such as Drug-protein complexes and also provides a better basis for the production of more efficient and newer drugs and vaccines as well as experimental and in silico approaches for researchers (Dareini et al. 2020; Sadeghzadeh et al. 2020). Molecular modeling approaches and determining the binding site and binding affinity in order to monitor and identify the binding sites between two protein or peptide complexes, can help to consciously and accurately select the desired epitopes to be used in the vaccine structure or design of peptide inhibitors (Danesh et al. 2018; Mokaberi et al. 2021). We designed a recombinant multi-epitope vaccine based on the potential of cellular immune response stimulation of three proprietary bladder cancer antigens, and TLR agonists, using immunoinformatics tools and then evaluated vaccine structure via protein–protein docking and molecular dynamics (MD) simulation. This study aimed to design a multiepitope recombinant vaccine based on bladder cancer antigens to investigate the specific stimulation of cellular immune system against bladder cancer.

Methodology

Protein Selection

Uniprot database-base was used to retrieve HUMAN B melanoma antigen 4 (BAGE4), HUMAN Bladder cancer-associated protein (BLCAP), and HUMAN Melanoma antigen preferentially expressed in tumors (PRAME) proteins based on anti-cancerous properties.

Prediction of Peptide-MHC Class I Binding

The NetMHC 4.0 server (http://www.cbs.dtu.dk/services/NetMHC/) was used to prediction of peptide-MHC class I binding molecules. This server is harnessing Artificial Neural Networks (ANN) capable of performing sensitive, quantitative predictions of peptide binding to the MHC class I molecule. The HLA-A, HLA-B and HLA-C MHC class I molecules were select for binding to antigens.

The Prediction of MHC Class II Alleles

We used the MHC-II-peptide binding affinity prediction methods to predict of MHC class II alleles. This server (http://www.cbs.dtu.dk/services/NetMHCII/) uses an extended data set of quantitative MHC-peptide binding affinity data obtained from the Immune Epitope Database. The Human alleles including DR, DP, and DQ were used for the prediction of MHC class II alleles.

Designing of Cancer Vaccine Construct

The AAY linker bonded CTL epitopes. The GGGS linker also fused HTL epitopes. The EAAAK linker was used to bind Human Beta-defensin 3 and BAGE4. Also, Beta-defensin and PADRE adjuvants were added to the N-terminal and C-terminal region of the construct, respectively. Finally, the amino acid structure of the bladder cancer vaccine was formed.

Physicochemical Properties, Primary, Secondary of the Construct

The theoretical properties of the construct were estimated using ProtParam (http://web.expasy.org/protparam).

Furthermore, PsiPred online software (http://bioinf.cs.ucl.ac.uk/psipred/) was used to predicts the secondary structure of the protein. PsiPred utilizes the self-optimized prediction method (SOPM) that defined based on the amino acid sequence.

Prediction of Antigenicity and Allergenicity

The rate of construct allergenicity was determined by AlgPred (http://www.imtech.res.in/raghava/algpred/). This server predicts the allergenicity of a protein with a sensitivity accuracy of about 85% (Saha and Raghava 2006). The predicting of the antigenic value of the construct was determined by the VaxiJen v2.0 server on (http://www.ddg-pharmfac.net/vaxijen/VaxiJen.html). VaxiJen v2.0 proposes a new alignment-free approach for antigen prediction to overcome the limitations of alignment-dependent methods, which is based on auto cross-covariance (ACC) transformation of protein sequences into uniform vectors of principal amino acid properties (Doytchinova and Flower 2007). The solubility of protein was evaluated via the SOLpro server (http://proteomics.ics.uci.edu). SOLpro is a server for protein secondary structure prediction based on protein evolutionary information (sequence homology) and homologous protein's secondary structure (structure homology) which achieves a performance exceeding 79% correctly classified residues on proteins with no homologs in the PDB and exceeding 92% correctly classified residues on proteins where homologs can be found in the PDB (Magnan et al. 2009).

In Silico Cloning and Optimization of Vaccine

Java Utility Server (JCat) (http://www.prodoric.de/JCat) was utilized for codon optimizing the recombinant cancer vaccine construct. The pET-26b(+) was selected as a protein-expressing vector. The sequence was optimized for expression in a negative gram bacteria *E. coli* K12. The *Nde* I and *Xho* I restriction enzymes were selected for restriction sites in the SnapGene tool.

The Prediction of Linear B-Cell Epitopes

The B-Cells epitopes were predicted using the IEDB server (https://www.iedb.org/). This server has collected methods to predict linear B-cell epitopes based on sequence characteristics of the antigen using amino acid scales and HMMs. B-Cells epitopes are one of the most important factors contributing to the vaccine design because they are characterized by the immune system.

The Prediction of Discontinuous B-Cell Epitopes

All discontinuous B cell epitopes were determined using the ElliPro server. The importance of these epitopes is due to their decisive role in the spatial form of antigenic structures (Ponomarenko et al. 2008). We developed a model with a prediction accuracy of more than 85% and Area Under the Curve (AUC) 0.9 via the ElliPro which uses the amino acid composition as an input feature for the Support Vector Machine (SVM).

Interaction Between of HLA Class I Peptides

GalaxyPepDock server was used to evaluate the interaction between the selected epitopes and HLA class I (Ko et al. 2012). Since HLA-A6823 was repeated for 12 of the total HLA class I epitopes of both BCAP and PRAME antigens (in Table 1), HLA-A6823-epitope was selected for docking (Crooke et al. 2020). The 3D structure of HLA-A6823 was modeled with 67% similarity to the crystal structure of HLA-B*1501 (RCSB code: 1xr9) and then docked with SMFMGFYLL, CTICALVFL, LWFSHSMFM, HSMFMGFYL, CTICALVFL, TLAKFSPYL, HVMNPLETL, YIAQFTSQF, KAMVQAWPF, FPPLFMAAF, RTFYDPEPI and LPRELFPPL epitopes. Results was evaluated based on protein structure similarity (TM-score) and Interaction similarity score. Ten models of each peptide-HLA complex were generated on the basis of minimized energy scores, and the top model for each complex was selected for comparative analysis.

Structure Modeling, Validation, and Refinement

I-Tasser modeled the 3D structure of the construct (Yang and Zhang 2015). I-TASSER server is an online platform that implements algorithms for protein structuring and function predictions. It allows us to automatically generate high-quality model predictions of the 3D structure and biological function of protein molecules from their amino acid sequences. The modeled construct of the cancer vaccine was refined by https://zhanglab.ccmb.med.umich.edu/ModRefiner. The Ramachandran plot graph and Z-Score were used to validate of modeled construct in http://molprobity.biochem.duke.edu/ and https://www.came.sbg.ac.at/prosa.php, respectively.

Protein–Protein Docking

We used the crystallographed structures of TLR2 and TLR7 which were selected based on their interaction with the bladder cancer antigens. Also, we selected the binding site TLR's receptor based on the binding site belonging to I-TASSER server information. Each of the TLR2 (6NIG

Table 1 MHC Class-I alleles molecules prediction

Peptide	HLA	Affinity (nM)	% Rank	Allergen	Toxin pred
BCAP					
SMFMGFYLL	HLA-A3207 HLA-A0201 HLA-A0202 HLA-A0206 HLA-A0211 HLA-A0212 HLA-A0216 HLA-A0217 HLA-A0219 HLA-A0250 HLA-A2301 HLA-A2402 HLA-A2902 HLA-A3201 HLA-A3215 HLA-A6823 HLA-B0801 HLA-B0802 HLA-B0803 HLA-B1502 HLA-B1503 HLA-B2720 HLA-B3801 HLA-B3901 HLA-B4013 HLA-B4801 HLA-C0401	7.83	0.08	Non-allergen	Non-toxin
YCLQWLLPV	HLA-A6901 HLA-A0211 HLA-A0205 HLA-A0212 HLA-A0216 HLA-A0217 HLA-A2603 HLA-A3207 HLA-A3215 HLA-A6601 HLA-B2720 HLA-C0802 HLA-C1203 HLA-C1502	9.31	0.05	Allergen	Non-toxin
FMGFYLLSF	HLA-B4601 HLA-B0802 HLA-B0801 HLA-A0250 HLA-A0211 HLA-A2301 HLA-A2501 HLA-A2902 HLA-A3201 HLA-A3215 HLA-A8001 HLA-B0803 HLA-B1402 HLA-B1501 HLA-B1502 HLA-B1503 HLA-B2720 HLA-B4013 HLA-C0702	230.45	0.02	Non-allergen	Non-toxin

Table 1 (continued)

Peptide	HLA	Affinity (nM)	% Rank	Allergen	Toxin pred
CTICALVFL	HLA-A6802 HLA-A2603 HLA-A2602 HLA-A0211 HLA-A6601 HLA-A6823 HLA-C1502	6.41	0.07	Allergen	Non-toxin
YSCWGNCFL	HLA-C0501 HLA-C0303 HLA-B1517 HLA-A0250 HLA-B3801 HLA-B3901 HLA-C1203	198.09	0.20	Allergen	Non-toxin
CYSCWGNCF	HLA-A2402 HLA-A2301 HLA-A2403 HLA-B4201 HLA-C0702 HLA-C1402	16.17	0.01	Allergen	Non-toxin
LWFSHSMFM	HLA-A2902 HLA-A2403 HLA-A6823 HLA-B4013 HLA-C0401 HLA-C0602 HLA-C0701 HLA-C1402	292.92	0.17	Non-allergen	Non-toxin
FSHSMFMGF	HLA-B1517 HLA-B0802 HLA-A2601 HLA-A2403 HLA-B1501 HLA-B1502 HLA-B1503 HLA-B5301	2.36	0.03	Non-allergen	Non-toxin
HSMFMGFYL	HLA-A6823 HLA-A6601 HLA-A6802 HLA-A6901 HLA-A3207 HLA-A3215	14.46	0.01	Non-allergen	Non-toxin
CTICALVFL	HLA-A6802 HLA-A6601 HLA-A6823 HLA-A2602 HLA-A2603 HLA-C1502	6.41	0.07	Allergen	Non-toxin
PRAME					

Table 1 (continued)

Peptide	HLA	Affinity (nM)	% Rank	Allergen	Toxin pred
NLTHVLYPV	HLA-A0212 HLA-A0216 HLA-A0201 HLA-A0202 HLA-A0203 HLA-A0206 HLA-A0207 HLA-A0211 HLA-A0217 HLA-A0219 HLA-A0250 HLA-A3215 HLA-A6601 HLA-A6802 HLA-A6901	2.81	0.01	Non-allergen	Non-toxin
TLAKFSPYL	HLA-A0217 HLA-A0201 HLA-A0202 HLA-A0203 HLA-A0205 HLA-A0212 HLA-A0216 HLA-A0219 HLA-A6823 HLA-A6901 HLA-C0401	23.88	0.02	Non-allergen	Non-toxin
FLRGRLDQL	HLA-B0802 HLA-A0202 HLA-A0203 HLA-A0211 HLA-A0216 HLA-A0250 HLA-B0801 HLA-B0803 HLA-B1402 HLA-C0602 HLA-C0701	7311.01	0.15	Non-allergen	Non-toxin
RLRELLCEL	HLA-A0250 HLA-A0202 HLA-A0203 HLA-A0211 HLA-A0212 HLA-A0216 HLA-A3207 HLA-A3001 HLA-B0803	8.05	0.12	Non-allergen	Non-toxin
HVMNPLETL	HLA-A6823 HLA-A3207 HLA-A0217 HLA-A2603 HLA-A3201 HLA-A3215 HLA-A6601 HLA-A6802 HLA-A6901	48.61	0.10	Non-allergen	Non-toxin

Table 1 (continued)

Peptide	HLA	Affinity (nM)	% Rank	Allergen	Toxin pred
YIAQFTSQF	HLA-A2501 HLA-A2403 HLA-A2601 HLA-A2602 HLA-A2603 HLA-A2902 HLA-A3215 HLA-A6601 HLA-A6823 HLA-B0803 HLA-B1501 HLA-B1502 HLA-B1503 HLA-B3501 HLA-B8301 HLA-B4601 HLA-C0501 HLA-C1203 HLA-C1402	163.39	0.02	Non-allergen	Non-toxin
KAMVQAWPF	HLA-A3201 HLA-A2403 HLA-A3207 HLA-A3215 HLA-A6823 HLA-B0803 HLA-B1503 HLA-B1517 HLA-B2720 HLA-B3501 HLA-B4013 HLA-B4601 HLA-B5701 HLA-B1503 HLA-B5801 HLA-B5802	4.55	0.01	Non-allergen	Non-toxin
FPPLFMAAF	HLA-B3503 HLA-A2501 HLA-A2602 HLA-A6823 HLA-B0802 HLA-B3501 HLA-B4201 HLA-B5101 HLA-B5301 HLA-B8301	445.62	0.01	Non-allergen	Non-toxin
RTFYDPEPI	HLA-A3207 HLA-A3201 HLA-A3215 HLA-A6802 HLA-A6823 HLA-B1503 HLA-B1517 HLA-B2720 HLA-B4013 HLA-B5801 HLA-C1502 HLA-C1203	10.62	0.01	Non-allergen	Non-toxin

Table 1 (continued)

Peptide	HLA	Affinity (nM)	% Rank	Allergen	Toxin pred
LPRELFPPL	HLA-B8301 HLA-C0401 HLA-B4201 HLA-B5101 HLA-B5401 HLA-B0702 HLA-B0801 HLA-B0802 HLA-B2720 HLA-B3501 HLA-B3503 HLA-A3207 HLA-A6823	338.83	0.01	Non-allergen	Non-toxin

PDB code) and TLR7 (7CYN PDB code) PDBs structures were retrieved from the RCSB server and saved. Then, structures of the TLR PDBs were minimized energy in the MVD software. All of the additional ligands and water molecules were deleted. In the next step, the cancer vaccine construct was introduced to MVD software and all the steps for docking preparation were performed like TLRs structures. Protein–protein docking was performed by the HADDOCK server. HADDOCK distinguishes itself from ab-initio docking methods in that it encodes information from identified or predicted protein interfaces in Ambiguous Interaction Restraints (AIRs) to drive the docking process. We defined amino acids identified in the previous step for interaction HADDOCK. Then, we selected the best cluster which had the most negative HADDOCK score after docking.

The Molecular Dynamics of the Protein–Protein Complex

MD simulation was utilized as an important technique for analyzing and investigating the protein–protein complex validation. GROMACS v.5.1.4 (http://manual.gromacs.org/documentation/5.1.4/index.html) was used to simulation of the construct-TLRs complexes. The system was neutralized by the addition of an appropriate concentration of sodium or chloride ions. Energy minimization was performed based on which this process was a descent steeped algorithm. System equilibration was performed for NVT and NPT ensemble that the temperature was then brought up to 300 K and 1 bar pressure. Simulation of complexes were carried out for the protein–protein by 40 ns time scale to analyze the trajectories after the equilibration process.

MM/BPSA Analysis

Contributions for the binding free energy of complexes were calculated by MM-PBSA analysis.

$$\Delta G\text{bind, solv} = \Delta G\text{bind, vaccum} + \Delta G\text{solv, complex} - (\Delta G\text{solv, ligand} + \Delta G\text{solv, complex}) \quad (1)$$

$$\Delta G\text{sol} = \text{Gelecterostatic}\epsilon = 80 - \text{Gelecterostatic} = 1 + \Delta G\text{hydrophobic} \quad (2)$$

$$\Delta G\text{vaccum} = \Delta E\text{molecular mechanics} - \text{T}.\Delta S\text{normal mode analysis} \quad (3)$$

Solvation free energies was determined via solving the linearised Poisson Boltzman equation for reaching the electrostatic contribution in the solvation free energy.

Average interaction energy between receptor, ligand and taking the entropy change upon binding into account was used to calculates ΔGvacuum.

Immune Simulation

Simulation of the immunological response excitation for constructed bladder vaccine was validated by the C-ImmSim server (http://150.146.2.1/C-IMMSIM/index.php). Three major functional mammal system components (bone marrow, thymus, and lymph node) are simulated in this server. The ability to simulate various types of immune cells such as CTL, HTL, B-cells, dendritic cells and cytokines was considered for this candidate bladder vaccine when it is made. The immune simulation was performed taking into account the minimum clinical interval between doses of two

vaccines, which is four weeks and using similar protocols reported by previous studies. For a total of 1050 steps of the simulation were administered three injections with the recommended intervals of four weeks. Other parameters were set as default.

Results

Protein Retrieval and Selection

All three proteins were stored in the FASTA form after retrieval in the Uniprot.

The Prediction of Cytotoxic T-Cell Lymphocyte Epitopes

NetMHC 4.0 server was used to predict MHC-I epitopes. As can be seen in Table 1, 20 Cytotoxic T-cell Lymphocyte epitopes (9-mer) were selected for HLA-A, HLA-B, and HLA-C of MHC Class-I alleles molecules based on most repeatability among strong binds. Those T-cell epitopes that had recurrence and overlap were identified and selected along with other T-cell epitopes for the construct. All MHC-I epitopes are included in supplementary Table S1.

The Prediction of Helper T Lymphocyte (HTL) Epitopes

The helper T lymphocyte (HTL) epitopes were predicted using NetMHC II 2.3 server. During this step, 10 Human MHC-II allele molecules, including DR, DP, and DQ were selected based on the most repeatability among strong binds. Each of the HTL epitopes molecules has defaulted to 15mer (with 9mer core) (Table 2). All investigated epitopes related to helper T lymphocyte are shown in Supplementary Table S2.

Designing of Protein Construct of Vaccine

We used complete BAGE4 protein sequence. The design of multiepitope bladder vaccine used 5 important factors. These items including 3 proteins, along with Beta-defensin 3 and PADRE adjuvants. Different linkers were used to fuse each of peptides. Beta-defensin 3 and PADRE were bonded using EAAAK linker. The connection among CTL peptides was performed using the AAY linker. Furthermore, the connection among HTL peptides was created via the GGGS linker (Fig. 1).

Physicochemical Properties, Primary, Secondary Structure

The results of ProtParam server showed that the bladder construct vaccine is protein, including 743 amino acids, the molecular weight of 82.18 kDa, theoretical isoelectric (pI) of about 9.44, Aliphatic Index of 83.15, and an Instability Index of 50.5. These results confirmed that the construct is a stable protein. Moreover, the Grand average of hydropathicity of this bladder peptide vaccine is 0.341. The construct has a half-life of about 30 h in mammalian reticulocytes (in vitro), > 20 h in yeast (in vivo), and > 10 h in *Escherichia coli* (in vivo). The secondary structure of bladder cancer construct is included in Supplementary Fig. S1.

In Silico Studies and Development of Bladder Vaccine

Two *Xho* I and *Nde* I restriction enzymes were selected for in silico cloning nucleotide sequence with the length of 2229 bp. The mean GC of sequences and codon compatibility index (CAI) of the nucleotide sequences was 52.26% and 1.0, respectively. Finally, because *E. coli* bacterium K12 will be amused as an expression host, the nucleotide sequence was cloned inside the pET26b (+) vector. HisTag was considered in the C-terminal sequence, and the final vaccine sequence was designed by SnapGene software (Fig. 2).

Homology Modeling, Refinement, Validation

I-Tasser server modeled the vaccine construct. Then, the modeled construct was submitted to the ModRefiner server for refining. TM score difference between the raw and refined structure was 0.46 angstrom, respectively. Using the ProSA server, the Z-score of construct was determined about −6.35 before refinement, while this value was obtained −6.9 after refinement (Fig. 3A, B). Ramachandran graph details indicated most of the amino acids which make up the model are in favored and allowed areas (%86.7 in favored regions, and 95.9% in allowed regions) (Fig. 3C, D). Favored regions allowed regions and outlier areas were calculated 91.9% and 98.2%, after refinement, respectively. Superimposition of bladder cancer vaccine structure, before and after the refinement, respectively (Fig. 3E).

The Prediction of Linear and Conformational B-Cell Epitopes of the Final Construct

B-cells epitopes of final construct were predicted using the IEDB server. As shown in Table 3, all predicted epitopes had an antigenicity greater than 0.4. In the next step, conformational B-cells epitopes for each of the peptides were predicted using the ElliPro server. Conformational B-cells

Table 2 MHC Class-II alleles molecules prediction

Peptide	HLA	Affinity (nM)	% Rank	Allergen	Toxin pred	IFN inducer	IL10 inducer
BCAP							
HSMFMGFYLLSFLLE	DRB1_0402 HLA-DPA10103-DPB10201 HLA-DQA10104-DQB10503 HLA-DPA10201-DPB10101 HLA-DPA10103-DPB10401 HLA-DPA10103-DPB10601 HLA-DQA10104-DQB10503	229.7	0.12	Non-allergen	Non-toxin	POSITIVE	IL10 inducer
SMFMGFYLLSFLLER	DRB1_0402 HLA-DQA10101-DQB10501 HLA-DQA10102-DQB10502 HLA-DQA10104-DQB10503 HLA-DPA10103-DPB10401 HLA-DPA10103-DPB10601 HLA-DPA10201-DPB10101 HLA-DPA10201-DPB10501 HLA-DPA10103-DPB10201	236.9	0.15	Non-allergen	Non-toxin	POSITIVE	IL10 inducer
SHSMFMGFYLLSFLL	DRB1_0402 HLA-DPA10103-DPB10401 HLA-DPA10103-DPB10601 HLA-DPA10103-DPB10201 HLA-DQA10104-DQB10503	251.5	0.20	Non-allergen	Non-toxin	POSITIVE	IL10 inducer
FSHSMFMGFYLLSFL	HLA-DPA10103DPB10201 DRB1_0402 HLA-DPA10103DPB10401 HLA-DPA10103DPB10601 HLA-DQA10104-DQB10503	12.6	0.20	Non-allergen	Non-toxin	POSITIVE	IL10 inducer
MFMGFYLLSFLLERK	HLA-DPA10103-DPB10601 DRB1_0402 HLA-DPA10103-DPB10401 HLA-DPA10201-DPB10101 HLA-DPA10201-DPB10501 HLA-DPA10103-DPB10201 HLA-DQA10102-DQB10502 HLA-DQA10104-DQB10503	2.7	0.12	Non-allergen	Non-toxin	POSITIVE	IL10 inducer
PALWFSHSMFMGFYL	HLA-DQA10601-DQB10402 HLA-DPA10103-DPB10401 DRB1_0402 DRB1_0701 HLA-DPA10103-DPB10402 HLA-DPA10103-DPB10402 HLA-DPA10301-DPB10402 HLA-DPA10103-DPB10201 HLA-DQA10201-DQB10402 HLA-DQA10501-DQB10302 HLA-DQA10501-DQB10302 HLA-DQA10601-DQB10402	29.1	0.10	Non-allergen	Non-toxin	POSITIVE	IL10 inducer
LNPALWFSHSMFMGF	HLA-DPA10103-DPB10401 DRB1_0402 DRB1_0701 HLA-DPA10103-DPB10402 HLA-DPA10103-DPB10601 HLA-DPA10103-DPB10201 HLA-DQA10201-DQB10402 HLA-DQA10601-DQB10402 HLA-DQA10601-DQB10402	12.8	0.40	Non-allergen	Non-toxin	POSITIVE	IL10 inducer

Table 2 (continued)

Peptide	HLA	Affinity (nM)	% Rank	Allergen	Toxin pred	IFN inducer	IL10 inducer
NPALWFSHSMFMGFY	HLA-DQA10601-DQB10402 HLA-DPA10103-DPB10401 DRB1_0402 DRB1_0701 HLA-DPA10103-DPB10402 HLA-DPA10103-DPB10601 HLA-DPA10103-DPB10201 HLA-DQA10201-DQB10402 HLA-DQA10501-DQB10302 HLA-DQA10601-DQB10402 HLA-DQA10501-DQB10302	26.6	0.09	Allergen	Non-toxin	POSITIVE	IL10 inducer
ALWFSHSMFMGFYLL	HLA-DPA10103-DPB10401 DRB1_0402 DRB1_0701 HLA-DPA10103-DPB10402 HLA-DPA10103-DPB10601 HLA-DPA10301-DPB10402 HLA-DPA10103-DPB10201 HLA-DQA10501-DQB10302 HLA-DQA10601-DQB10402	7.3	0.12	Non-allergen	Non-toxin	POSITIVE	IL10 inducer
FMGFYLLSFLLERKP	HLA-DPA10103-DPB10601 DRB1_0402 HLA-DPA10103-DPB10401 HLA-DPA10201-DPB10101 HLA-DPA10201-DPB10501 HLA-DPA10103-DPB10201 HLA-DQA10101-DQB10501 HLA-DQA10102-DQB10502 HLA-DQA10104-DQB10503	2.6	0.09	Non-allergen	Non-toxin	POSITIVE	IL10 inducer
PRAME							
SRYISMSVWTSPRRL	HLA-DQA10601-DQB10402 HLA-DQA10201-DQB10402 DRB4_0103 DRB4_0103 DRB1_0101 DRB1_0404 DRB1_0405 DRB1_1001	33.2	0.15	Non-allergen	Non-toxin	POSITIVE	IL10 inducer
YLIEKVKRKKNVLRL	DRB1_1301 DRB4_0103 DRB5_0101 DRB4_0103 DRB5_0101 DRB1_1301 DRB1_1101 DRB1_0103	2.6	0.12	Non-allergen	Non-toxin	POSITIVE	IL10 inducer
SYLIEKVKRKKNVLR	DRB1_1301 DRB4_0103 DRB5_0101 DRB1_1301 DRB4_0103 DRB5_0101 DRB1_0103 DRB1_1101	2.6	0.12	Non-allergen	Non-toxin	POSITIVE	IL10 inducer

Table 2 (continued)

Peptide	HLA	Affinity (nM)	% Rank	Allergen	Toxin pred	IFN inducer	IL10 inducer
LRRLLLSHIHASSYI	DRB1_1201 DRB4_0103 DRB1_1301 DRB4_0101 HLA-DPA10103-DPB10301 HLA-DQA10102-DQB10602 HLA-DQA10104-DQB10503 DRB1_0401 DRB1_0404 DRB1_0701 DRB1_1101	28.4	0.40	Non-allergen	Non-toxin	NEGATIVE	IL10 inducer
NLRRLLLSHIHASSY	DRB4_0101 DRB4_0103 DRB1_1301 HLA-DPA10103-DPB10301 HLA-DQA10102-DQB10602 DRB1_0401 DRB1_0404 DRB1_1101 DRB1_1201	14.4	0.30	Non-allergen	Non-toxin	POSITIVE	IL10 inducer
LERLAYLHARLRELL	DRB1_1301 DRB4_0103 DRB5_0101 HLA-DQA10501-DQB10402 HLA-DPA10103-DPB10301 HLA-DQA10303-DQB10402 DRB1_0701 DRB1_0801 DRB1_0901	3.5	0.30	Non-allergen	Non-toxin	POSITIVE	IL10 inducer
ERLAYLHARLRELLC	DRB1_1301 DRB4_0103 DRB5_0101 HLA-DQA10501-DQB10402 HLA-DQA10303-DQB10402 DRB1_0701 DRB1_0801 DRB1_0901	3.5	0.30	Non-allergen	Non-toxin	POSITIVE	IL10 inducer
HLERLAYLHARLREL	DRB4_0103 DRB5_0101 DRB1_1301 HLA-DQA10501-DQB10402 HLA-DPA10103-DPB10301 HLA-DQA10303-DQB10402 DRB1_0701 DRB1_0801	4.3	0.40	Non-allergen	Non-toxin	POSITIVE	IL10 inducer
CCKKLKIFAMPMQDI	DRB4_0101 DRB1_1501 HLA-DPA10201-DPB11401 HLA-DPA10103-DPB10301 HLA-DQA10401-DQB10402 HLA-DQA10102-DQB10602 DRB1_1001 DRB1_1201	7.9	0.05	Non-allergen	Non-toxin	POSITIVE	IL10 inducer

Table 2 (continued)

Peptide	HLA	Affinity (nM)	% Rank	Allergen	Toxin pred	IFN inducer	IL10 inducer
QCLQALYVDSLFFLR	HLA-DPA10301-DPB10402 HLA-DPA10103-DPB10201 DRB3_0101 HLA-DPA10103-DPB10401 HLA-DPA10201-DPB10101 HLA-DQA10101-DQB10501 HLA-DQA10104-DQB10503 HLA-DQA10501-DQB10201	18.7	0.50	Non-allergen	Non-toxin	POSITIVE	IL10 inducer

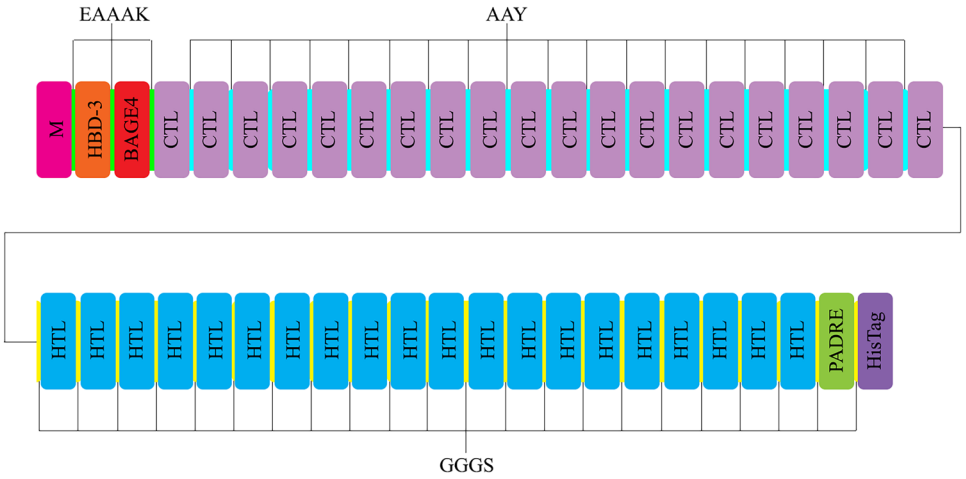

Fig. 1 Graphical representation of bladder cancer vaccine construct

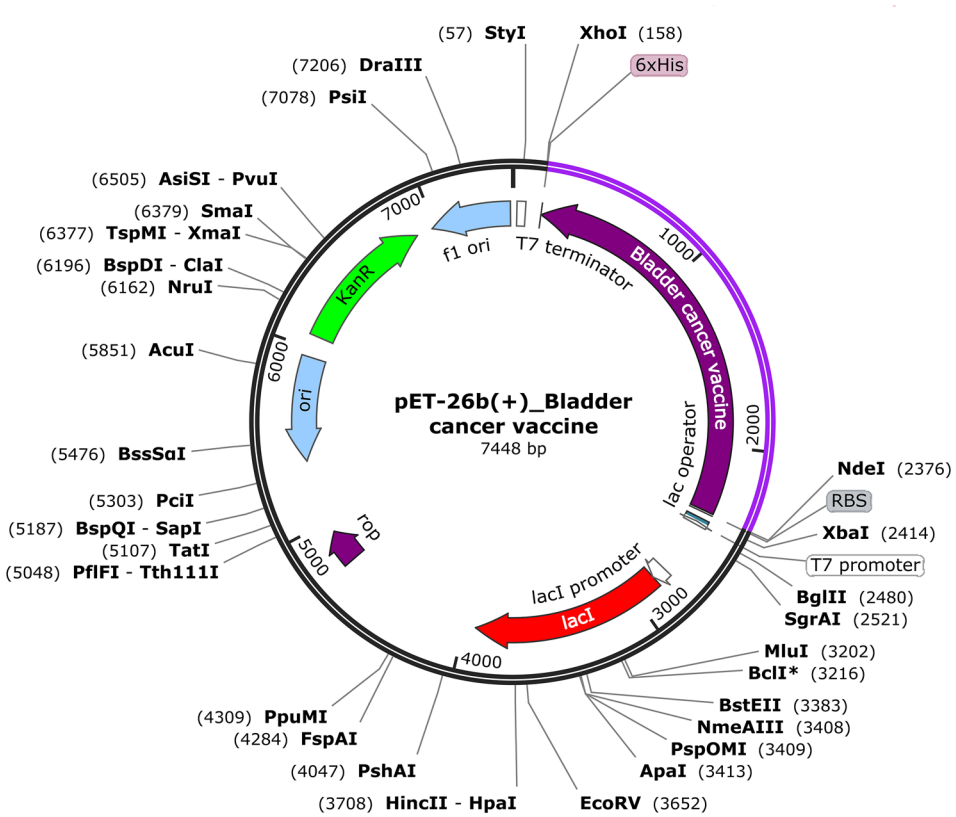

Fig. 2 In silico cloning of bladder vaccine nucleotide sequence to pET26b by SnapGene

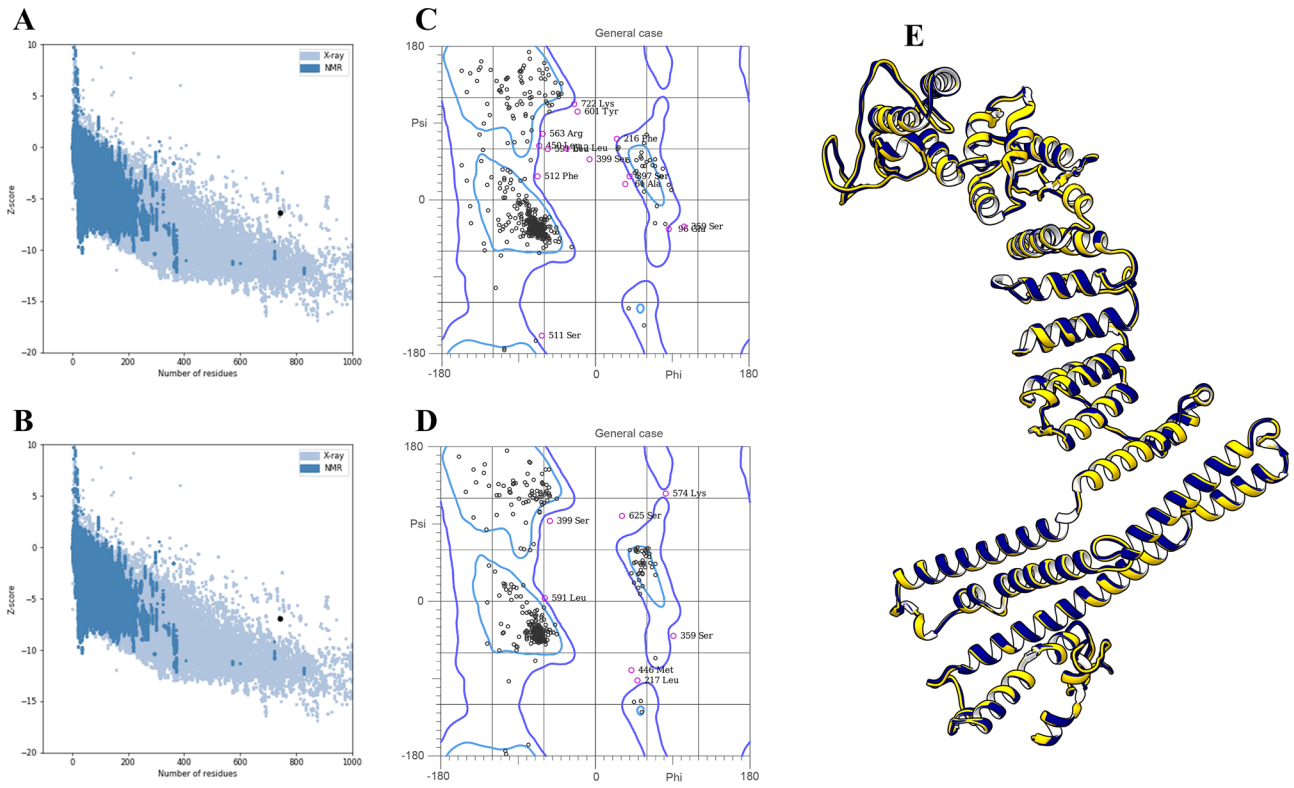

Fig. 3 Modeling, refinement and validation of bladder cancer vaccine 3D structure. **A** and **B** Z-Score of bladder cancer vaccine 3D structure, before and after structure refinement. **C** and **D** Ramachandran graph related to bladder cancer vaccine 3D structure, before and after structure refinement. **E** Superimposition of modeled to bladder cancer vaccine 3D structure. Blue structure is referred to before refinement and yellow structure is referred to after refinement

Table 3 B-cell epitopes selected from final construct

Length	Start	End	Peptide	Antigenicity
24	31	54	PKEEQIGKCSTRGRKC-CRRKKEAA	0.9630
6	319	324	YDPEPI	0.8204
12	329	340	PRELFPPLGGGS	0.6794
6	374	379	RGGGSS	2.9492
6	430	435	RKGGGS	1.6665
8	524	531	RKPGGGSS	1.4637
12	539	550	WTSPRRLGGGSY	0.4402
14	574	587	KVKRKKNVLRGGGS	1.6643
7	600	606	SYIGGGS	0.9922
6	640	645	LGGGSE	3.0637
9	693	701	PMQDIGGGS	0.7765
7	734	740	GGGSHHH	2.8971

epitopes selected for the final construct are shown in Supplementary Table S3.

Binding Characteristics of HLA Class I Peptide with HLA-A6823

The HLA class I candidate peptides were predicted to provide the highest coverage in the HLA-A6823 allele. Because the HLA-A6823 was the only candidate to show the most connection to class 1 epitopes (with 12 repetitions), with a relatively high affinity. Therefore, we performed the molecular binding studies of each peptide with the molecular structure of HLA-A6823. The results showed that all peptides bind in the peptide binding groove (Fig. 4 and Table 4). Binding of epitopes in the hydrophobic binding cavity of the HLA groove supports the hypothesis that these peptides

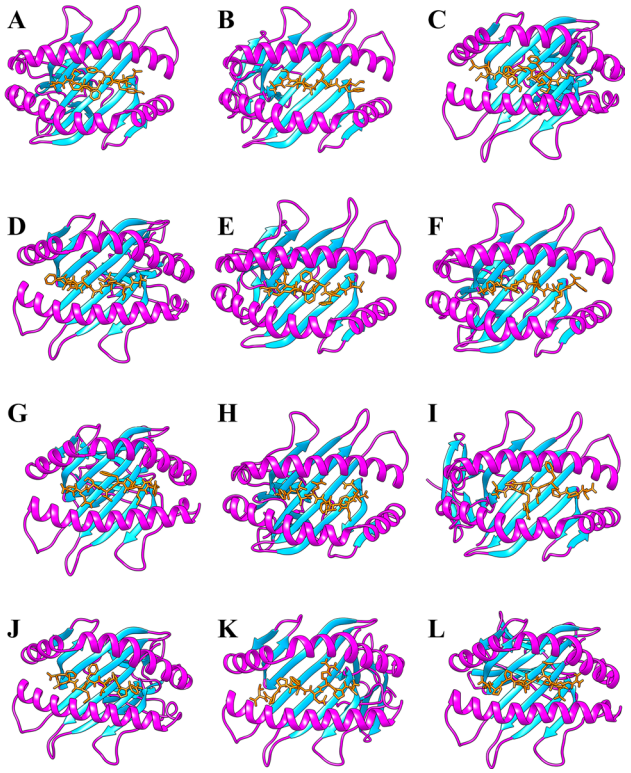

Fig. 4 MHC-I: Epitope interaction. **A** HLA-A6823: SMFMGFYLL, **B** HLA-A6823: CTICALVFL, **C** HLA-A6823: LWFSHSMFM, **D** HLA-A6823: HSMFMGFYL, **E** HLA-A6823: CTICALVFL, **F** HLA-A6823: TLAKFSPYL, **G** HLA-A6823: HVMNPLETL, **H** HLA-A6823: YIAQFTSQF, **I** HLA-A6823: KAMVQAWPF, **J** HLA-A6823: FPPLFMAAF, **K** HLA-A6823: RTFYDPEPI and **L** HLA-A6823: LPRELFPPL. HLA-A6823 is shown as purple and blue. Epitopes are shown as orang ligands

Table 4 Template modeling and interaction similarity scores related to the most repetitive MHC-I epitopes for HLA-A6823

Peptide sequence	Protein structure similarity (TM-score)	Interaction similarity score
SMFMGFYLL	0.981	210.0
CTICALVFL	0.978	202.0
LWFSHSMFM	0.982	218.0
HSMFMGFYL	0.977	211.0
CTICALVFL	0.979	238.0
TLAKFSPYL	0.983	224.0
HVMNPLETL	0.977	205.0
YIAQFTSQF	0.956	200.0
KAMVQAWPF	0.979	231.0
FPPLFMAAF	0.962	223.0
RTFYDPEPI	0.985	219.0
LPRELFPPL	0.979	214.0

Table 5 HADDOCK results related to bladder vaccine-TLR2 complex

HADDOCK score	− 43.4 ± 21.4
Cluster size	6
RMSD from the overall lowest-energy structure	0.8 ± 0.5
Van der Waals energy	− 58.7 ± 7.2
Electrostatic energy	− 196.8 ± 68.2
Desolvation energy	29.2 ± 7.2
Restraints violation energy	254.8 ± 21.97
Buried surface area	1807.8 ± 222.2
Z-score	− 2.1

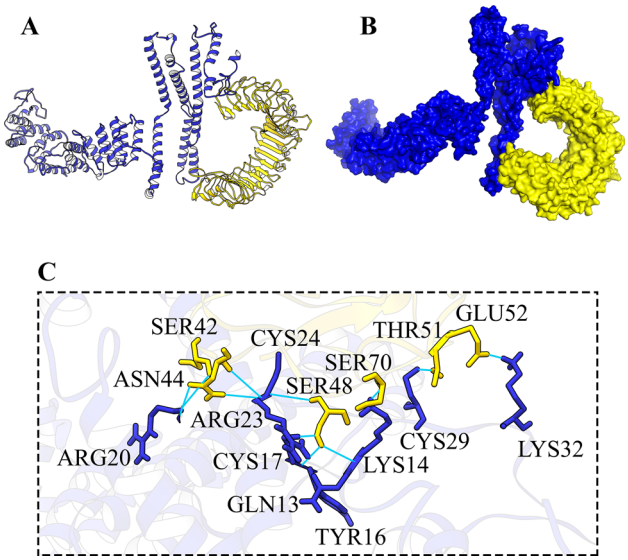

Fig. 5 HADDOCK docking results of bladder vaccine-TLR2 complex. **A** Bladder vaccine-TLR2 complex is shown as ribbons. **B** Bladder vaccine-TLR2 complex is shown as surface. **C** Bladder vaccine-TLR2 complex is shown as magnified sticks. Bladder vaccine structure is blue and TLR2 structure is yellow

Table 6 HADDOCK results related to bladder vaccine-TLR7 complex

HADDOCK score	− 107.6 ± 12.0
Cluster size	79
RMSD from the overall lowest-energy structure	20.2 ± 0.3
Van der Waals energy	− 80.5 ± 2.9
Electrostatic energy	− 214.7 ± 47.1
Desolvation energy	− 10.7 ± 16.3
Restraints violation energy	266.0 ± 26.59
Buried surface area	2300.4 ± 82.5
Z-score	− 2.1

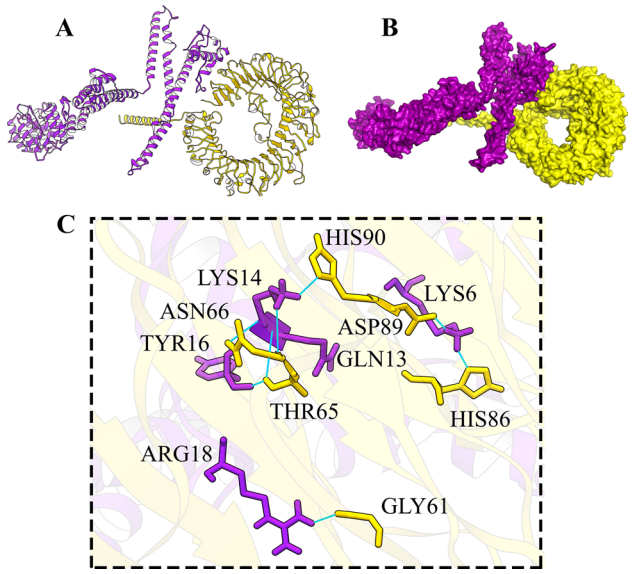

Fig. 6 HADDOCK docking results of bladder vaccine-TLR7 complex. **A** Bladder vaccine-TLR7 complex is shown as ribbons. **B** Bladder vaccine-TLR7 complex is shown as surface. **C** Bladder vaccine-TLR7 complex is shown as magnified sticks. Bladder vaccine structure is purple and TLR7 structure is yellow

bind strongly to HLA-A6823 and could be promising epitope candidates for vaccine development studies and if used in the structure of the vaccine, they can induce an appropriate immune response.

Protein–Protein Docking

In the first step, the raw 3D structure of bladder cancer vaccine was minimized by MVD software. Then, the bladder cancer vaccine and TLRs were introduced to HADDOCK server for docking. Each protein–protein docking was separately performed (vaccine-TLR2 and vaccine-TLR7). HADDOCK score in the bladder vaccine-TLR2 complex was obtained − 40 (Table 5) (Fig. 5A–C), moreover, the docking results of HADDOCK server showed the best complex with a HADDOCK score of -104 there are in the vaccine-TLR7 complex (Table 6) (Fig. 6A–C). All of the interactions between vaccines and TLRs are shown as 2D in Fig. 7A, B.

Molecular Dynamic

The MD simulation method performs interactions between the protein/protein, such as vaccine/receptor analysis. The structural integrity of vaccine-TLR2 and vaccine-TLR7 docked complexes were simulated via 35 ns by MD. Then, MD's results, such as root-mean square-deviations (RMSD) was used followed for the analysis of hydrogen bonds interaction between bladder vaccine structure and TLRs. As shown in Fig. 8A, RMSD graph relates to the vaccine-TLR7 complex indicated an upward trend; however, after 5 ns, it has almost stabilized. Vaccine-TLR2 and vaccine-TLR7 complexes had an RMSD average value of about 2.5 and 2.2 nm after the complexes stabilized, respectively. RMSD results is inferred that the vaccine-TLR2 and vaccine-TLR7 complexes remained stable via 35 ns simulations. Root mean-square-fluctuations (RMSF) were calculated to further calculations of residual and side-chain flexibility of complexes (Figs. 8B and 9B). Almost no obvious fluctuations in complexes, nonetheless fluctuations at the amino acid interaction regions up to 0.4 nm, but the other complexes residues remained highly stable in their fluctuations. The results of MD simulation endorse that referring to the HADDOCK docking, this vaccine could strongly evoke a significant immune response against TLRs related to bladder cancer. Furthermore, the Radius of gyration related to vaccine-TLR2 and vaccine-TLR7 complexes (~ 1.5–1.4) showed the potential of stability maintenance in complexes (Figs. 8C and 9C). Also, H-bond graphs in vaccine-TLR2 and vaccine-TLR7 complexes are remained unchanged via the MD, indicating that the complexes remain stable (Figs. 8D and 9D).

MM/BPSA Analysis

MD results were more evaluated by MM/BPSA analysis to determine the energy contribution of involved amino acids in each complex. As shown in Table 8, the energy contribution of vaccine-TLR7 complex is higher than vaccine-TLR2 (Table 7). Besides, further analysis indicates van der Waal energy is negative in both complexes, but vaccine-TLR7 complex shows higher negative electrostatic energy compare to vaccine-TLR2. In general, MM/BPSA analysis showed a better interaction in vaccine-TLR7 complex, although overall results of docking, MD simulation, and MM/BPSA analysis confirm high stable interaction for vaccine-TLR2 and vaccine-TLR7 complexes.

Immune Simulation

Real-life phenomena adequation was achieved based on the response of in silico mediated immune. As shown in Fig. 10A, the primary reaction was lower than both secondary and tertiary reactions, which follows rapid antigen clearance leads to the distinguishing of the immunoglobulin movement greater such as IgM, IgG1 + IgG2, and IgG + IgM antibodies. Significant development of memory cells is shown that is relevant to a higher activation level of B-cells with IgM and IgG1 biotype (Fig. 10B, C). In the next context, the number of elicited active T-cells by the bladder vaccine was enhanced throughout the secondary or tertiary reactions, but gradually decreased after that (Fig. 10D–G). Bladder cancer vaccine simulations lead to evoke immune responses as well as significantly increased levels of

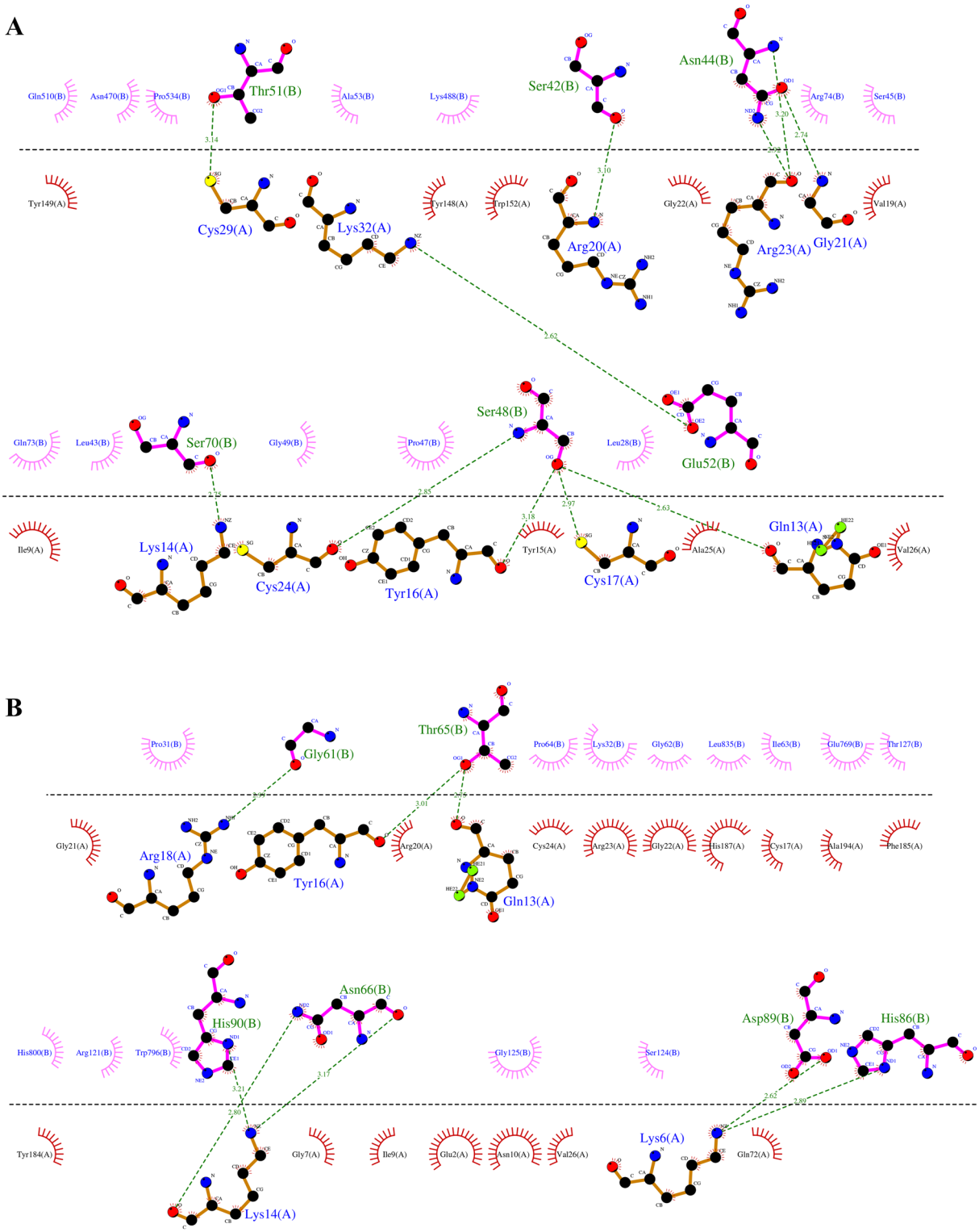

Fig. 7. 2D presentation of HADDOCK results. **A** Bladder vaccine-TLR2 complex. Bladder vaccine amino acids are shown as orange sticks and TLR2 amino acids are shown as pink sticks. **B** Bladder vaccine-TLR7 complex. Bladder vaccine amino acids are shown as orange sticks and TLR7 amino acids are shown as pink sticks

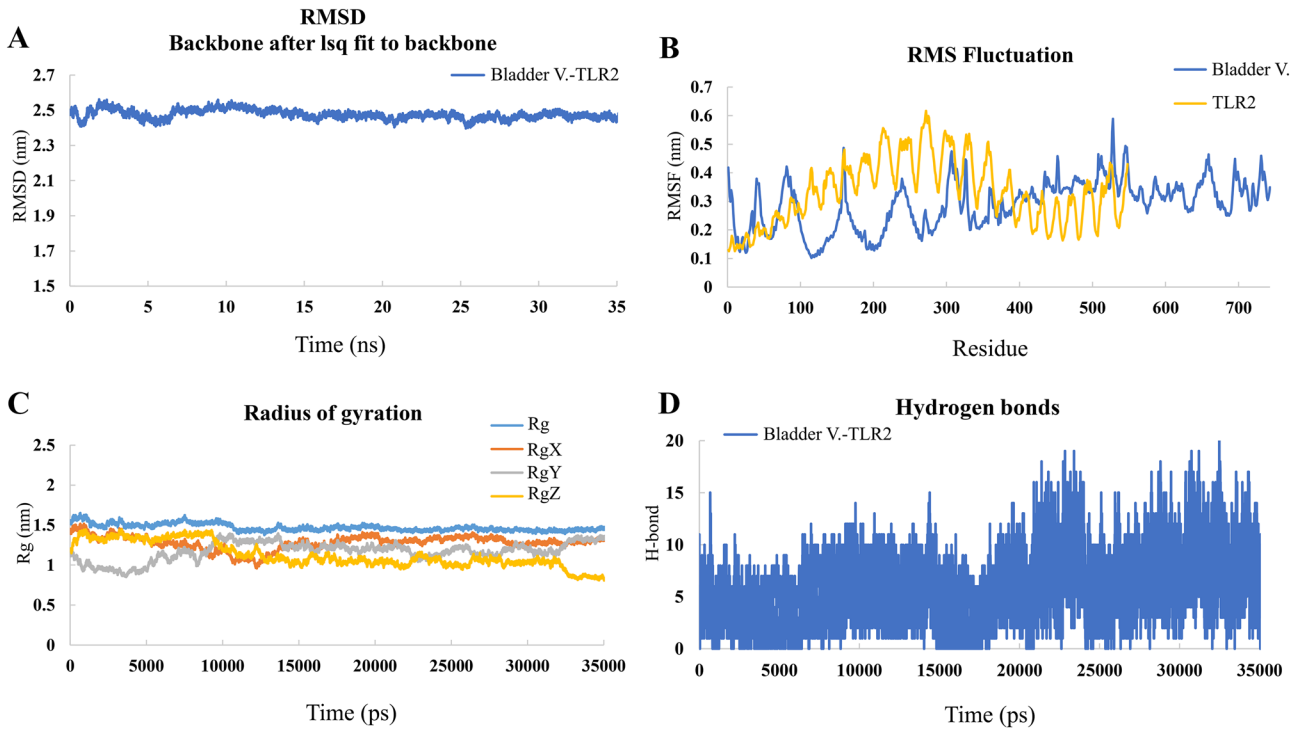

Fig. 8 MD simulation results of bladder vaccine-TLR2 complex. **A** RMSD, **B** RMSF, **C** Rg and **D** Hydrogen bonds graphs related to bladder vaccine-TLR2 complex

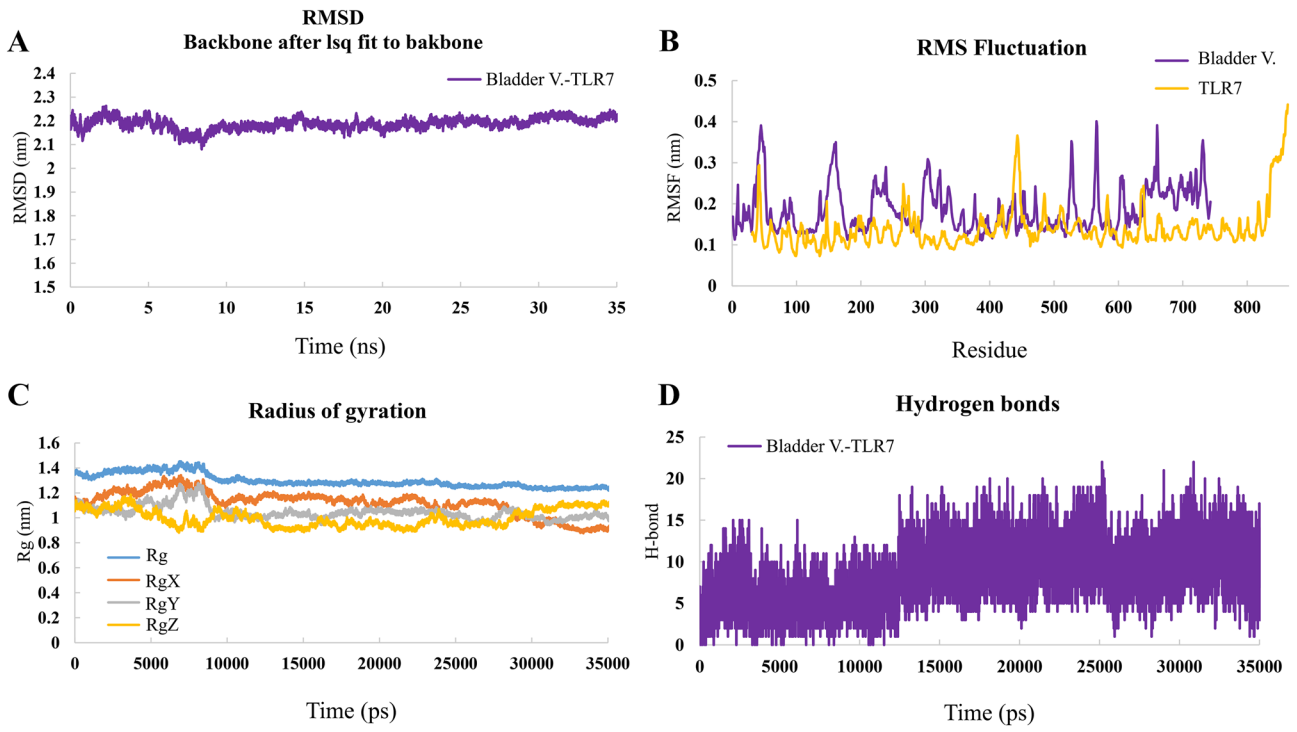

Fig. 9 MD simulation results of bladder vaccine-TLR7 complex. **A** RMSD, **B** RMSF, **C** Rg and **D** Hydrogen bonds graphs related to bladder vaccine-TLR7 complex

Table 7 MM/PBSA analysis related to bladder vaccine-TLR2 complex

MM/PBSA-complexes	Bladder vaccine-TLR2 complex
van der Waal energy	− 84.298 ± 119.222 kJ/mol
Electrostatic energy	91.399 ± 34.605 kJ/mol
Polar solvation energy	138.601 ± 177.082 kJ/mol
SASA energy	− 11.613 ± 13.675 kJ/mol
Binding energy	134.088 ± 24.857 kJ/mol

Table 8 MM/PBSA analysis related to bladder vaccine-TLR7 complex

MM/PBSA-complexes	Bladder vaccine-TLR7 complex
van der Waal energy	− 346.800 ± 28.646 kJ/mol
Electrostatic energy	− 1069.632 ± 41.093 kJ/mol
Polar solvation energy	879.497 ± 57.964 kJ/mol
SASA energy	− 42.517 ± 1.567 kJ/mol
Binding energy	− 579.452 ± 36.709 kJ/mol

dendritic cells, T-regulatory cells, and macrophages, and also cytokines like IFN-γ and IL-2 (Fig. 10H–L). Results of prediction and simulation of immune response originated from bladder cancer injection in C-IMMSIM showed this vaccine can produce promising anti-cancerous immune reactions.

Discussion

Despite significant advances in cancer treatment today, cancer is still one of the leading causes of death worldwide. Most cancer treatment regimens for the treatment of choice for advanced or metastatic disease steps have originated focus primarily on chemotherapy (Schirrmacher 2019). The overall quality of life in the patients undergoing chemotherapy is decreased under affecting the wide range of side effects generated by high toxicity and induce from Current chemotherapeutic drugs (Yin et al. 2016). Furthermore, a wide range from chemotherapeutic agents is identified and expelled by those cancer cells which display a high tendency to develop resistance against chemotherapeutic compounds (Schirrmacher 2019).

Traditional methods of designing a cancer vaccine are costly and time-consuming tasks requiring many experimental studies (Fatoba et al. 2022). Today, due to the advent of computational biology methods such as genomics, proteomics, and immunoinformatics tools, the ability to construct, predict, and interact a virtual cancer vaccine with immune system molecules has been achieved. It is not possible to analyze these benefits in traditional vaccine production methods. The rapid development of computational methods and models, along with a vast body of experimental data to analyze the immune system response using immunological data, has led to the simulation of immune system response to the cancer vaccine (Aminnezhad et al. 2020).

Using cancer vaccines is more effective than current treatments for cancer, including chemotherapy and radiation, especially for treating melanoma-related cancers such as bladder cancer. Activating and stimulating the immune system against specific antigens to elicit an anti-tumor immune response using a vaccine is the great purpose of immunization against cancer. Numerous studies showed that using different types of antigens associated with melanoma-related tumors, has yielded excellent results for vaccination (Boël et al. 1995; Ruault et al. 2002, 2003; Weber et al. 2011; Al-Khadairi and Decock 2019; Safavi et al. 2019; Ellingsen et al. 2021; Ouyang et al. 2021; Richard et al. 2021). We used BLCAP, PRAM, and BAGE4 antigens as key factors in our construct. Regarding the expression of BLCAP, PRAM, and BAGE4 in malignant tissues, these antigens could potentially be used as appropriate targets for anticancer immunization (Moreira et al. 2010; Gordeeva 2018; Lezcano et al. 2018; Lohman et al. 2021). Although so far there is no report that simultaneously examines the interaction between the three antigens BLCAP, PRAM and BAGE4 in physiological conditions and the interaction behavior among them in vivo; However, a number of studies have shown that each of the three antigens BLCAP, PRAM, and BAGE4 may have an interaction partner in bladder or testis cancer separately (Cho et al. 2006; Chen et al. 2017; Gromova et al. 2017). For example, Gromova et al. (2017) showed that BLCAP and Stat3 are in close physical proximity of each other in bladder tissue, and that BLCAP physically interacts with Stat3, so that BLCAP is a novel Stat3 interaction partner and suggested a role for BLCAP in the Stat3-mediated progression of precancerous lesions to invasive tumors of the bladder. BLCAP plays a role as a novel STAT3 interaction partner in bladder cancer. Functional association for each of the antigens can be associated with concomitant and same direction responses to elicit immune responses (Gromova et al. 2017).

The selected region was fused to the CTL epitopes by GGGS linker to facilitate the delivery of epitopes via MHC processing and effective fragment separation. CTLs play a vital role in the cell's immune response to cancer by inducing apoptosis in tumor cells as well as producing interferon-gamma (Yong et al. 2012). The stimulation of CTL epitopes was the most important parameter to select BLCAP, PRAM, and BAGE4 antigens.

An appropriate vaccine should be able to stimulate helper T lymphocyte (HTL) responses to achieve maximum efficacy. HTL-related responses can play a key role to regulate a wide range from different immune system responses. Stimulation of HTL can trigger the production of memory T

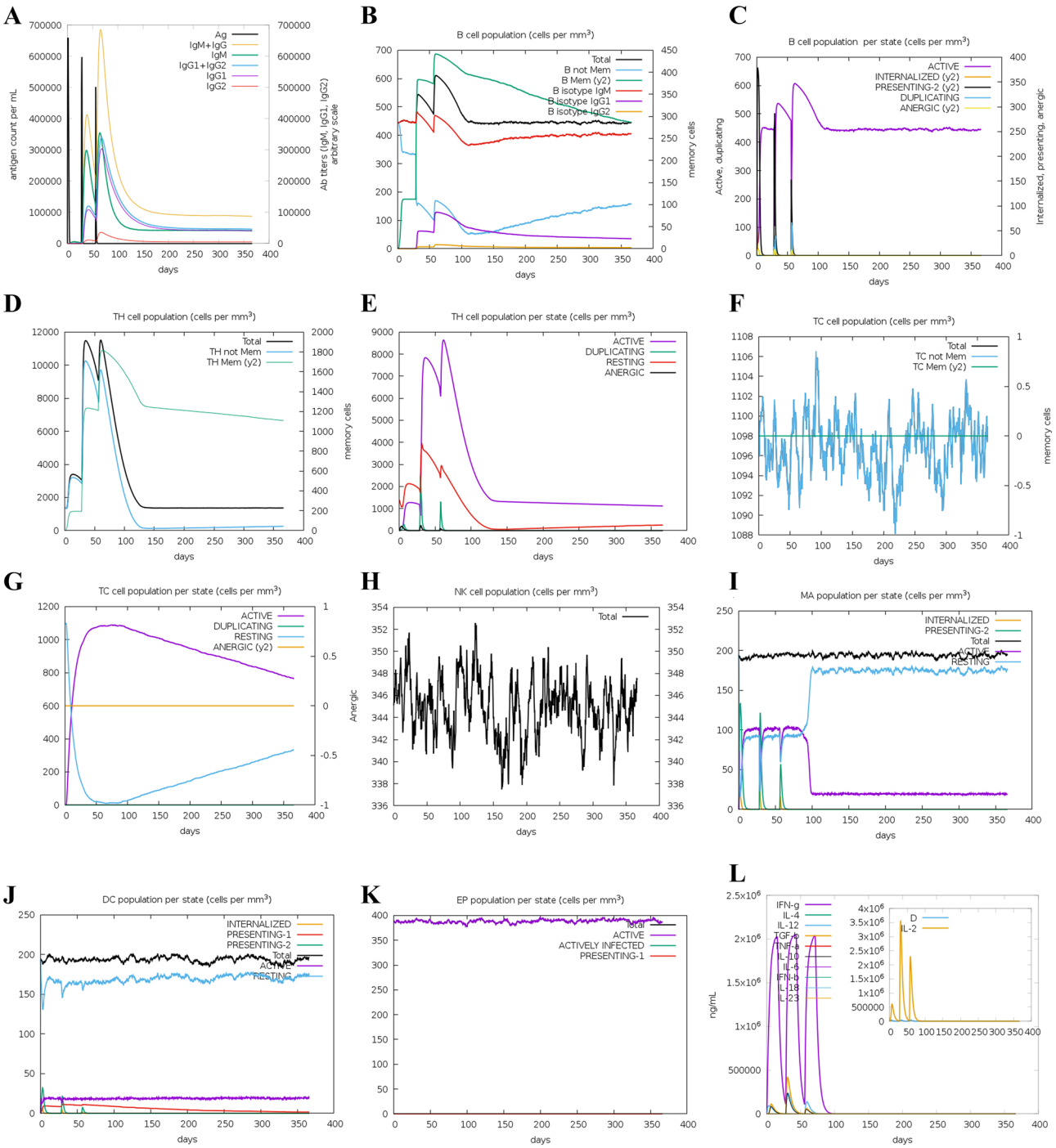

Fig. 10 Immune simulation after bladder cancer vaccine injection. **A** Antigen and immunoglobulins, **B** B lymphocytes: total count, memory cells, and sub-divided in isotypes IgM, IgG1 and IgG2, **C** B-lymphocytes population per entity-state (i.e., showing counts for active, presenting on class-II, internalized the Ag, duplicating and anergic, **D** CD4 T-helper lymphocytes count. The plot shows total and memory counts **E** CD4 T-helper lymphocytes count sub-divided per entity-state (i.e., active, resting, anergic and duplicating), **F** CD8 T-cytotoxic lymphocytes count. Total and memory shown, **G** CD8 T-cytotoxic lymphocytes count per entity-state, **H** Natural Killer cells (total count), **I** Dendritic cells. DC can present antigenic peptides on both MHC Class-I and class-II molecules. The curves show the total number broken down to active, resting, internalized and presenting the ag, **J** Macrophages. Total count, internalized, presenting on MHC class-II, active and resting macrophages, **K** Epithelial cells. Total count broken down to active, virus-infected and presenting on Class-I MHC molecule, **L** Cytokines. Concentration of cytokines and interleukins. D in the inset plot is danger signal

cells and the activation of dendritic cells, respectively (Nezafat et al. 2014). Besides, HTL can initiate and maintain an immune response against the tumor. BLCAP, PRAM, and BAGE4 antigens were used to adequately stimulate HTL epitopes.

20 CTL epitopes and 20 HTL epitopes derived from BLCAP and PRAM antigens were fused by AAY and GGGS linkers, respectively. Besides, we considered and BAGE4 sequence as an independent antigen. In addition to activating HTL, these linkers maintain vaccine-dependent immunogenicity for the CTL response. Beta-defensin 3 and PADER sequence selected in this study are considered the detectable adjuvants for the Toll-like receptor (TLR) that activate the cellular immune response (Funderburg et al. 2007; Ferris et al. 2013). The integration of these adjuvants into the structure of cancer vaccine could increase its effectiveness, as TLRs are important in identifying pathogens by various immune cells, including B cells, dendritic cells, and macrophages (Adams 2009). The activation of TLRs by their specific adjuvants can increase the secretion of inflammatory cytokines and the over-regulation of MHC molecules. The activation of TLRs, in addition to differentiating simple HTL cells from T-helper1, leads to the activation of CTLs (Kawai and Akira 2007). Therefore, choosing the right agonist to stimulate TLR can greatly enhance the success of the immune response elicited by the cancer vaccine. Beta-defensin 3 is a well-known agonist for stimulating TLR complex. The interaction of Beta-defensin with TLRs leads dendritic cells to T-helper1 cells and subsequently stimulates cellular immune responses (Safavi et al. 2019). The Beta-defensin was fused to the BAGE4 via EAAAK linkers. EAAAK, as a helical structure, was placed in the C-terminal of Beta-defensin to reduce its interaction with other peptide vaccine domains. The presence of an EAAAK linker can spatially separate B and T cell epitopes and ultimately lead to proper vaccine interaction with TLRs. B cells affect dendritic cells, natural killer cells, and myeloid-suppressing cells that express Fc receptors by producing antibodies and forming antigen–antibody complexes (Xu-Monette and Young 2020). Furthermore, the mechanism of antibody-dependent cell-mediated cytotoxicity is one of the most important strengths of B cells in the elimination of cancer cells (Zappasodi et al. 2015; Xu-Monette and Young 2020). Since the selected MHC-I and MHC-II epitopes provided maximum antigen coverage for the vaccine, we selected B-cell epitopes from the final sequence of the vaccine to prevent the vaccine structure from over-enlarging. As expected, the overall antigenicity of B cell epitopes from the final structure of the vaccine was very significant. Considering the importance of the fact that B cells are very important in responding to the multi-peptide peptide vaccine, 12 linear B cell epitopes were selected from the final construct that showed the highest antigenicity. Moreover, conformational B cell epitopes were identified on the amino acid sequence of the vaccine. Considering this strategy for the cancer vaccine by determining a large number of B cell epitopes leads to an effective humoral immune response in the body. The high solubility of structure after protein expression increases stability and immunogenicity. The final structure is codon-optimized to maximize expression in the prokaryotic host. The final DNA structure was integrated into the pET26b vector to in silico cloning of bladder cancer vaccine. In addition, studies have shown that protein folding is influenced by physicochemical properties, so understanding intermolecular relationships, such as protein complexes, can improve the prediction of molecular structures (Chamani and Moosavi-Movahedi 2006). Regarding bladder cancer immunotherapy, Galluzzi et al. (2012) showed that TLR2 signaling is strongly stimulated through BCG therapy (Galluzzi et al. 2012). This finding confirms that appropriate stimulation of TLR2 may occur if antigen-specific antigens are used. Phase II studies of the CDX-1307 bladder cancer vaccine have also demonstrated the activation of TLR signaling pathways in patients with newly diagnosed bladder cancer (Morse et al. 2011). Alignment of laboratory results and bioinformatics simulations can increase the reliability of studies. Application of molecular modeling in the study of Zare-Feizabadi et al. (2021) in the interaction of calf thymus DNA (ct DNA) with anastrozole (which is acknowledged as an antineoplastic drug), supported and confirmed anti-cancer results of anastrozole use on MCF 7 cell line (Zare-Feizabadi et al. 2021). TLR2 represents a double-edged sword whose role in cancer must be carefully understood in order to launch effective therapies. Because it is expressed in various malignancies and promotes their proliferation through activation of the myeloid differentiation primary response protein 88 (MyD88)/nuclear factor kappa-light-chain-enhancer of activated B cell (NF-κB) pathway. Hence, to activate immune responses, TLR2 is considered as a player in anti-cancer immunity. Therefore, TLR2 agonists have been used as adjuncts to anti-cancer immunotherapies. Anticancer inhibitors or agonists induce apoptosis or death of cancer cells by activating immune pathways (Moosavi-Movahedi et al. 2003; Di Lorenzo et al. 2020).

Docking results showed a high affinity between Bladder cancer vaccine structure and both of TLR2/TLR7. Then docking results were evaluated by MD simulation to confirmation of structure interactions. As it was identified, MD simulation confirmed the stability of both bladder vaccine-TLR2 and bladder vaccine-TLR7 by RMSD, RMSF, Rg graphs. Furthermore, MM/PBSA analysis indicated high negative energy contributions of amino acids in complexes, as well as electrostatics and Van der Waals energy. Using docking techniques and MD simulations, the results of immune responses at the cellular and molecular levels can be used before laboratory tests to evaluate cancer vaccines.

Conclusion

Using prevention methods, such as multi-epitope vaccines containing antigens expressed in bladder cancer can provide effective immunity against bladder cancer. The MHC-I and MHC-II epitopes selected from BLCAP and PRAM antigens had the highest coverage in the final structure of the vaccine. B cell epitopes were selected and identified from the final structure of the vaccine that had high antigenicity to induce hemorrhagic immunity. In addition, the interaction of HLA class I molecules with MHC-I epitopes indicated that high-affinity peptides were expected to be used to develop specific vaccines against bladder cancer. As shown in our study, the bladder cancer vaccine candidate can establish strong interactions with prognostic molecules such as TLR2 and TLR7. Therefore, studies simulating the immune responses given to this vaccine showed that both humoral and cellular immune responses are evoked.

Supplementary Information The online version contains supplementary material available at https://doi.org/10.1007/s10989-022-10380-7.

Acknowledgements None

Author Contributions Conceptualization, EJ and GhAJ; methodology, EJ, GhAJ, MN and AM; formal analysis, EJ and GhAJ; resources, MN and AM; data curation, EJ, GhAJ, MN and AM; writing—original draft preparation, EJ, GhAJ, MN and AM; writing—review and editing, EJ and GhAJ; project administration, EJ and GhAJ; funding acquisition, EJ and GhAJ. All authors have read and agreed to the published version of the manuscript.

Declarations

Conflict of interest None.

References

Adams S (2009) Toll-like receptor agonists in cancer therapy. Immunotherapy 1:949–964

Al-Khadairi G, Decock J (2019) Cancer testis antigens and immunotherapy: where do we stand in the targeting of PRAME? Cancers 11:984

Amin MB (2009) Histological variants of urothelial carcinoma: diagnostic, therapeutic and prognostic implications. Mod Pathol 22(Suppl 2):S96-s118

Aminnezhad S, Abdi-Ali A, Ghazanfari T, Bandehpour M, Zarrabi M (2020) Immunoinformatics design of multivalent chimeric vaccine for modulation of the immune system in *Pseudomonas aeruginosa* infection. Infect Genet Evol 85:104462

Beg AZ, Farhat N, Khan AU (2021) Designing multi-epitope vaccine candidates against functional amyloids in *Pseudomonas aeruginosa* through immunoinformatic and structural bioinformatics approach. Infect Genet Evol 93:104982

Bellizzi AM (2020) An algorithmic immunohistochemical approach to define tumor type and assign site of origin. Adv Anat Pathol 27:114–163

Berezney R, Buchholtz LA (1981) Dynamic association of replicating DNA fragments with the nuclear matrix of regenerating liver. Exp Cell Res 132:1–13

Bevers RF, Kurth KH, Schamhart DH (2004) Role of urothelial cells in BCG immunotherapy for superficial bladder cancer. Br J Cancer 91:607–612

Bian T, Li H, Zhou Q, Ni C, Zhang Y, Yan F (2017) Human β-defensin 3 reduces TNF-α-induced inflammation and monocyte adhesion in human umbilical vein endothelial cells. Mediators Inflamm 2017:8529542–8529542

Boël P, Wildmann C, Sensi ML, Brasseur R, Renauld JC, Coulie P, Boon T, Van Der Bruggen P (1995) BAGE: a new gene encoding an antigen recognized on human melanomas by cytolytic T lymphocytes. Immunity 2:167–175

Chamani J, Moosavi-Movahedi AA (2006) Effect of *n*-alkyl trimethylammonium bromides on folding and stability of alkaline and acid-denatured cytochrome c: a spectroscopic approach. J Colloid Interface Sci 297:561–569

Chen W, He W, Cai H, Hu B, Zheng C, Ke X, Xie L, Zheng Z, Wu X, Wang H (2017) A-to-I RNA editing of BLCAP lost the inhibition to STAT3 activation in cervical cancer. Oncotarget 8:39417–39429

Chi H, Li C, Zhao FS, Zhang L, Ng TB, Jin G, Sha O (2017) Anti-tumor activity of toll-like receptor 7 agonists. Front Pharmacol 8:10. https://doi.org/10.3389/fphar.2017.00304

Cho HJ, Caballero OL, Gnjatic S, Andrade VC, Colleoni GW, Vettore AL, Outtz HH, Fortunato S, Altorki N, Ferrera CA, Chua R, Jungbluth AA, Chen YT, Old LJ, Simpson AJ (2006) Physical interaction of two cancer-testis antigens, MAGE-C1 (CT7) and NY-ESO-1 (CT6). Cancer Immun 6:12

Crooke SN, Ovsyannikova IG, Kennedy RB, Poland GA (2020) Immunoinformatic identification of B cell and T cell epitopes in the SARS-CoV-2 proteome. Sci Rep 10:14179

Danesh N, Navaee Sedighi Z, Beigoli S, Sharifi-Rad A, Saberi MR, Chamani J (2018) Determining the binding site and binding affinity of estradiol to human serum albumin and holo-transferrin: fluorescence spectroscopic, isothermal titration calorimetry and molecular modeling approaches. J Biomol Struct Dyn 36:1747–1763

Dareini M, AmiriTehranizadeh Z, Marjani N, Taheri R, Aslani-Firoozabadi S, Talebi A, NayebzadehEidgahi N, Saberi MR, Chamani J (2020) A novel view of the separate and simultaneous binding effects of docetaxel and anastrozole with calf thymus DNA: experimental and in silico approaches. Spectrochim Acta Part A 228:117528

De Backer O, Arden KC, Boretti M, Vantomme V, De Smet C, Czekay S, Viars CS, De Plaen E, Brasseur F, Chomez P, Van Den Eynde B, Boon T, Van Der Bruggen P (1999) Characterization of the GAGE genes that are expressed in various human cancers and in normal testis. Cancer Res 59:3157–3165

De Plaen E, Traversari C, Gaforio JJ, Szikora J-P, De Smet C, Brasseur F, Van Der Bruggen P, Lethé B, Lurquin C, Chomez P, De Backer O, Boon T, Arden K, Cavenee W, Brasseur R (1994) Structure, chromosomal localization, and expression of 12 genes of the MAGE family. Immunogenetics 40:360–369

Degeorge KC, Holt HR, Hodges SC (2017) Bladder cancer: diagnosis and treatment. Am Fam Physician 96:507–514

Di Lorenzo A, Bolli E, Tarone L, Cavallo F, Conti L (2020) Toll-like receptor 2 at the crossroad between cancer cells, the immune system, and the microbiota. Int J Mol Sci 21:9418

Doytchinova IA, Flower DR (2007) VaxiJen: a server for prediction of protective antigens, tumour antigens and subunit vaccines. BMC Bioinform 8:4

Dyrskjøt L, Zieger K, Kissow Lildal T, Reinert T, Gruselle O, Coche T, Borre M, Ørntoft TF (2012) Expression of MAGE-A3,

NY-ESO-1, LAGE-1 and PRAME in urothelial carcinoma. Br J Cancer 107:116–122
Ellingsen EB, Mangsbo SM, Hovig E, Gaudernack G (2021) Telomerase as a target for therapeutic cancer vaccines and considerations for optimizing their clinical potential. Front Immunol. https://doi.org/10.3389/fimmu.2021.682492
Fang JY, Huang ZR (2009) Intravesical drug delivery into the bladder to treat cancers. Curr Drug Deliv 6:227–237
Fatoba DO, Amoako DG, Abia ALK, Essack SY (2022) Transmission of antibiotic-resistant *Escherichia coli* from chicken litter to agricultural soil. Front Environ Sci. https://doi.org/10.3389/fenvs.2021.751732
Feng CC, Wang PH, Guan M, Jiang HW, Wen H, Ding Q, Wu Z (2011) Urinary BLCA-4 is highly specific for detection of bladder cancer in Chinese Han population and is related to tumour invasiveness. Folia Biol (praha) 57:242–247
Ferris LK, Mburu YK, Mathers AR, Fluharty ER, Larregina AT, Ferris RL, Falo LD Jr (2013) Human beta-defensin 3 induces maturation of human langerhans cell-like dendritic cells: an antimicrobial peptide that functions as an endogenous adjuvant. J Invest Dermatol 133:460–468
Funderburg N, Lederman MM, Feng Z, Drage MG, Jadlowsky J, Harding CV, Weinberg A, Sieg SF (2007) Human-defensin-3 activates professional antigen-presenting cells via Toll-like receptors 1 and 2. Proc Natl Acad Sci USA 104:18631–18635
Galluzzi L, Vacchelli E, Eggermont A, Fridman WH, Galon J, Sautès-Fridman C, Tartour E, Zitvogel L, Kroemer G (2012) Trial watch: experimental toll-like receptor agonists for cancer therapy. Oncoimmunology 1:699–716
Getzenberg RH, Konety BR, Oeler TA, Quigley MM, Hakam A, Becich MJ, Bahnson RR (1996) Bladder cancer-associated nuclear matrix proteins. Cancer Res 56:1690–1694
Gordeeva O (2018) Cancer-testis antigens: Unique cancer stem cell biomarkers and targets for cancer therapy. Semin Cancer Biol 53:75–89
Gromova I, Svensson S, Gromov P, Moreira JMA (2017) Identification of BLCAP as a novel STAT3 interaction partner in bladder cancer. PLoS ONE 12:e0188827
Hennessy EJ, Parker AE, O'neill LJ (2010) Targeting Toll-like receptors: emerging therapeutics? Nat Rev Drug Discov 9:293–307
Hosseini S, Chamani J, Hadipanah MR, Ebadpour N, Hojjati AS, Mohammadzadeh MH, Rahimi HR (2019) Nano-curcumin's suppression of breast cancer cells (MCF7) through the inhibition of cyclinD1 expression. Breast Cancer (Dove Med Press) 11:137–142
Jiang Y, Yang D, Li W, Wang B, Jiang Z, Li M (2012) Antiviral activity of recombinant mouse β-defensin 3 against influenza A virus in vitro and in vivo. Antivir Chem Chemother 22:255–262
Jiang DM, Chung P, Kulkarni GS, Sridhar SS (2020) Trimodality therapy for muscle-invasive bladder cancer: recent advances and unanswered questions. Curr Oncol Rep 22:14
Joly S, Organ CC, Johnson GK, Mccray PB Jr, Guthmiller JM (2005) Correlation between beta-defensin expression and induction profiles in gingival keratinocytes. Mol Immunol 42:1073–1084
Kawai T, Akira S (2007) TLR signaling. Semin Immunol 19:24–32
Khandelwal P, Abraham SN, Apodaca G (2009) Cell biology and physiology of the uroepithelium. Am J Physiol Renal Physiol 297:F1477–F1501
Kim J, Yang YL, Jang S-H, Jang Y-S (2018) Human β-defensin 2 plays a regulatory role in innate antiviral immunity and is capable of potentiating the induction of antigen-specific immunity. Virol J 15:124
Ko J, Park H, Heo L, Seok C (2012) GalaxyWEB server for protein structure prediction and refinement. Nucleic Acids Res 40:W294–W297
Koch GE, Smelser WW, Chang SS (2021) Side effects of intravesical BCG and chemotherapy for bladder cancer: what they are and how to manage them. Urology 149:11–20
Kulkarni P, Shiraishi T, Rajagopalan K, Kim R, Mooney SM, Getzenberg RH (2012) Cancer/testis antigens and urological malignancies. Nat Rev Urol 9:386–396
Larue H, Ayari C, Bergeron A, Fradet Y (2013a) Toll-like receptors in urothelial cells-targets for cancer immunotherapy. Nat Rev Urol 10:537–545
Larue H, Ayari C, Bergeron A, Fradet Y (2013b) Toll-like receptors in urothelial cells—targets for cancer immunotherapy. Nat Rev Urol 10:537–545
Lenis AT, Lec PM, Chamie K, Mshs MD (2020) Bladder cancer: a review. JAMA 324:1980–1991
Lerut E, Van Poppel H, Joniau S, Gruselle O, Coche T, Therasse P (2015) Rates of MAGE-A3 and PRAME expressing tumors in FFPE tissue specimens from bladder cancer patients: potential targets for antigen-specific cancer immunotherapeutics. Int J Clin Exp Pathol 8:9522–9532
Lethé B, Lucas S, Michaux L, De Smet C, Godelaine D, Serrano A, De Plaen E, Boon T (1998) LAGE-1, a new gene with tumor specificity. Int J Cancer 76:903–908
Lezcano C, Jungbluth AA, Nehal KS, Hollmann TJ, Busam KJ (2018) PRAME expression in melanocytic tumors. Am J Surg Pathol 42:1456–1465
Lohman ME, Steen AJ, Grekin RC, North JP (2021) The utility of PRAME staining in identifying malignant transformation of melanocytic nevi 48:856–862
Magnan CN, Randall A, Baldi P (2009) SOLpro: accurate sequence-based prediction of protein solubility. Bioinformatics 25:2200–2207
Melekos MD, Moutzouris GD (2000) Intravesical therapy of superficial bladder cancer. Curr Pharm Des 6:345–359
Mokaberi P, Babayan-Mashhadi F, Zadeh AT, Saberi MR, Chamani J (2021) Analysis of the interaction behavior between Nano-Curcumin and two human serum proteins: combining spectroscopy and molecular stimulation to understand protein-protein interaction. J Biomol Struct Dyn 39:3358–3377
Moosavi-Movahedi AA, Hakimelahi S, Chamani J, Khodarahmi GA, Hassanzadeh F, Luo F-T, Ly TW, Shia K-S, Yen C-F, Jain ML, Kulatheeswaran R, Xue C, Pasdar M, Hakimelahi GH (2003) Design, synthesis, and anticancer activity of phosphonic acid diphosphate derivative of adenine-containing butenolide and its water-soluble derivatives of paclitaxel with high antitumor activity. Bioorg Med Chem 11:4303–4313
Moreira JMA, Ohlsson G, Gromov P, Simon R, Sauter G, Celis JE, Gromova I (2010) Bladder cancer-associated protein, a potential prognostic biomarker in human bladder cancer. MCP 9:161–177
Morse MA, Bradley DA, Keler T, Laliberte RJ, Green JA, Davis TA, Inman BA (2011) CDX-1307: a novel vaccine under study as treatment for muscle-invasive bladder cancer. Expert Rev Vaccines 10:733–742
Nezafat N, Ghasemi Y, Javadi G, Khoshnoud MJ, Omidinia E (2014) A novel multi-epitope peptide vaccine against cancer: an in silico approach. J Theor Biol 349:121–134
Nikpoor AR, Tavakkol-Afshari J, Gholizadeh Z, Sadri K, Babaei MH, Chamani J, Badiee A, Jalali SA, Jaafari MR (2015) Nanoliposome-mediated targeting of antibodies to tumors: IVIG antibodies as a model. Int J Pharm 495:162–170
Ohadian Moghadam S, Nowroozi MR (2019) Toll-like receptors: the role in bladder cancer development, progression and immunotherapy. Scand J Immunol 90:e12818
Ouyang X, Liu Y, Zhou Y, Guo J, Wei T-T, Liu C, Lee B, Chen B, Zhang A, Casey KM, Wang L, Kooreman NG, Habtezion A, Engleman EG, Wu JC (2021) Antitumor effects of iPSC-based cancer vaccine in pancreatic cancer. Stem Cell Rep 16:1468–1477

Ponomarenko J, Bui HH, Li W, Fusseder N, Bourne PE, Sette A, Peters B (2008) ElliPro: a new structure-based tool for the prediction of antibody epitopes. BMC Bioinform 9:514

Richard G, De Groot AS, Steinberg GD, Garcia TI, Kacew A, Ardito M, Martin WD, Berdugo G, Princiotta MF, Balar AV, Sweis RF (2021) Multi-step screening of neoantigens' HLA- and TCR-interfaces improves prediction of survival. Sci Rep 11:9983

Romih R, Korosec P, De Mello Jr. W, Jezernik K (2005) Differentiation of epithelial cells in the urinary tract. Cell Tissue Res 320:259–268

Ruault M, Van Der Bruggen P, Brun M-E, Boyle S, Roizès G, Sario AD (2002) New BAGE (B melanoma antigen) genes mapping to the juxtacentromeric regions of human chromosomes 13 and 21 have a cancer/testis expression profile. Eur J Hum Genet 10:833–840

Ruault M, Ventura M, Galtier N, Brun ME, Archidiacono N, Roizès G, De Sario A (2003) BAGE genes generated by juxtacentromeric reshuffling in the Hominidae lineage are under selective pressure. Genomics 81:391–399

Sadeghzadeh F, Entezari AA, Behzadian K, Habibi K, Amiri-Tehranizadeh Z, Asoodeh A, Saberi RM, Chamani J (2020) Characterizing the binding of angiotensin converting enzyme I inhibitory peptide to human hemoglobin: influence of electromagnetic fields. Protein Pept Lett 27:1007–1021

Safavi A, Kefayat A, Abiri A, Mahdevar E, Behnia AH, Ghahremani F (2019) In silico analysis of transmembrane protein 31 (TMEM31) antigen to design novel multiepitope peptide and DNA cancer vaccines against melanoma. Mol Immunol 112:93–102

Saha S, Raghava GPS (2006) AlgPred: prediction of allergenic proteins and mapping of IgE epitopes. Nucleic Acids Res 34:W202–W209

Santoni M, Catanzariti F, Minardi D, Burattini L, Nabissi M, Muzzonigro G, Cascinu S, Santoni G (2012) Pathogenic and diagnostic potential of BLCA-1 and BLCA-4 nuclear proteins in urothelial cell carcinoma of human bladder. Adv Urol 2012:397412

Schirrmacher V (2019) From chemotherapy to biological therapy: a review of novel concepts to reduce the side effects of systemic cancer treatment (review). Int J Oncol 54:407–419

Seddighzadeh M, Larsson P, Ulfgren AC, Onelöv E, Berggren P, Tribukait B, Torstensson A, Norming U, Wijkström H, Linder S, Steineck G (2003) Low IL-1alpha expression in bladder cancer tissue and survival. Eur Urol 43:362–368

Semple F, Webb S, Li HN, Patel HB, Perretti M, Jackson IJ, Gray M, Davidson DJ, Dorin JR (2010) Human beta-defensin 3 has immunosuppressive activity in vitro and in vivo. Eur J Immunol 40:1073–1078

Shelley MD, Court JB, Kynaston H, Wilt TJ, Fish RG, Mason M (2000) Intravesical bacillus calmette-guerin in Ta and T1 bladder cancer. Cochrane Database Syst Rev 2000:Cd001986

Shore ND, Palou Redorta J, Robert G, Hutson TE, Cesari R, Hariharan S, Rodriguez Faba O, Briganti A, Steinberg GD (2021) Non-muscle-invasive bladder cancer: an overview of potential new treatment options. Urol Oncol 39:642–663

Simpson AJG, Caballero OL, Jungbluth A, Chen Y-T, Old LJ (2005) Cancer/testis antigens, gametogenesis and cancer. Nat Rev Cancer 5:615–625

Slovacek H, Zhuo J, Taylor JM (2021) Approaches to non-muscle-invasive bladder. Cancer 23:105

So EY, Ouchi T (2010) The application of Toll like receptors for cancer therapy. Int J Biol Sci 6:675–681

Tani K, Murphy WJ, Chertov O, Salcedo R, Koh CY, Utsunomiya I, Funakoshi S, Asai O, Herrmann SH, Wang JM, Kwak LW, Oppenheim JJ (2000) Defensins act as potent adjuvants that promote cellular and humoral immune responses in mice to a lymphoma idiotype and carrier antigens. Int Immunol 12:691–700

Urban-Wojciuk Z, Khan MM, Oyler BL, Fåhraeus R, Marek-Trzonkowska N, Nita-Lazar A, Hupp TR, Goodlett DR (2019) The role of TLRs in anti-cancer immunity and tumor rejection. Front Immunol. https://doi.org/10.3389/fimmu.2019.02388

Validi M, Karkhah A, Prajapati VK, Nouri HR (2018) Immuno-informatics based approaches to design a novel multi epitope-based vaccine for immune response reinforcement against Leptospirosis. Mol Immunol 104:128–138

Van Eekelen CA, Van Venrooij WJ (1981) hnRNA and its attachment to a nuclear protein matrix. J Cell Biol 88:554–563

Vasekar M, Degraff D, Joshi M (2016) Immunotherapy in bladder cancer. Curr Mol Pharmacol 9:242–251

Veranic P, Romih R, Jezernik K (2004) What determines differentiation of urothelial umbrella cells? Eur J Cell Biol 83:27–34

Weber JS, Vogelzang NJ, Ernstoff MS, Goodman OB, Cranmer LD, Marshall JL, Miles S, Rosario D, Diamond DC, Qiu Z, Obrocea M, Bot A (2011) A phase 1 study of a vaccine targeting preferentially expressed antigen in melanoma and prostate-specific membrane antigen in patients with advanced solid tumors. J Immunother 34:556–567

Wołącewicz M, Hrynkiewicz R, Grywalska E, Suchojad T, Leksowski T, Roliński J, Niedźwiedzka-Rystwej P (2020) Immunotherapy in bladder cancer: current methods and future perspectives. Cancers 12:1181

Xu Y, Zou R, Wang J, Wang Z-W, Zhu X (2020) The role of the cancer testis antigen PRAME in tumorigenesis and immunotherapy in human cancer. Cell Prolif 53:e12770–e12770

Xu-Monette ZY, Young KH (2020) Therapeutic Vaccines for Aggressive B-Cell Lymphoma 61:3038–3051

Yang J, Zhang Y (2015) I-TASSER server: new development for protein structure and function predictions. Nucleic Acids Res 43:W174-181

Yin M, Joshi M, Meijer RP, Glantz M, Holder S, Harvey HA, Kaag M, Fransen Van De Putte EE, Horenblas S, Drabick JJ (2016) Neoadjuvant chemotherapy for muscle-invasive bladder cancer: a systematic review and two-step meta-analysis. Oncologist 21:708–715

Yong X, Xiao Y-F, Luo G, He B, Lü M-H, Hu C-J, Guo H, Yang S-M (2012) Strategies for enhancing vaccine-induced CTL antitumor immune responses. J Biomed Biotechnol 2012:605045–605045

Yu D-S, Wu C-L, Ping S-Y, Keng C, Shen K-H (2015) Bacille Calmette-Guerin can induce cellular apoptosis of urothelial cancer directly through toll-like receptor 7 activation. Kaohsiung J Med Sci 31:391–397

Zappasodi R, De Braud F, Di Nicola M (2015) Lymphoma immunotherapy: current status. Front Immunol. https://doi.org/10.3389/fimmu.2015.00448

Zare-Feizabadi N, Amiri-Tehranizadeh Z, Sharifi-Rad A, Mokaberi P, Nosrati N, Hashemzadeh F, Rahimi HR, Saberi MR, Chamani J (2021) Determining the interaction behavior of calf thymus DNA with anastrozole in the presence of histone H1: spectroscopies and cell viability of MCF-7 cell line investigations. DNA Cell Biol 40:1039–1051